

waterloopkundig laboratorium  
delft hydraulics laboratory

development of vibration-free gate design:  
learning from experience and theory

P. A. Kolkman

---

publication no. 219

November 1979

---

development of vibration-free gate design:  
learning from experience and theory

paper presented at the Symposium on  
Practical Experiences with Flow-Induced  
Vibrations,  
Karlsruhe, September, 3-6, 1979

P. A. Kolkman

---

publication no. 219

November 1979

DEVELOPMENT OF VIBRATION-FREE GATE DESIGN:  
LEARNING FROM EXPERIENCE AND THEORY

P.A. Kolkman

Head of the Locks, Weirs and Sluices Branch  
of the Delft Hydraulics Laboratory and  
Senior Research Officer at the  
Delft University of Technology

SUMMARY

Gate vibrations experienced by the author can be classified into three types:

- Vibration modes with flow-gap width variation due to gate vibration.
- Vibration modes with constant flow-gap width; often high-frequency plate vibrations are observed.
- Vibrations occurring at gate positions where the flow is wavering between reattachment and full separation.

The first type can be analysed theoretically. In the other two types, self-exciting vibration is probably due to a mechanism involving a fluctuating discharge coefficient, induced by the "added mass flow" of the vibrating gate (i.e. velocities in phase with the vibratory movement).

Different experiences concerning dynamic phenomena due to flow instability, sometimes amplified by partial aeration, are presented. One example demonstrates how a dangerous case of flow separation instability could not be reliably reproduced in a hydraulic model.

Finally, criteria for vibration-free gate design are formulated. The paper is followed by 12 illustrative charts concerning vibrations encountered in prototypes and in hydroelastic models.

1. INTRODUCTION

This paper contains cases from our experience, both practical and theoretical, with flow-induced gate vibrations in prototypes and hydraulic models. This will be presented in such manner that some generally applicable design criteria can be deduced.

Limitation to our own experiences has, on the one hand, the disadvantage that they come in at random and do not afford a complete picture of what may happen. On the other hand, the personal approach and incompleteness are more likely to provoke discussion. I also hope to convey some of the pleasures of pioneering in the field of flow-induced vibrations, which lies between the specialized branches of applied structural mechanics and fluid mechanics.

2. CONCLUSIONS FROM THE APPLIED STRUCTURAL MECHANICS

The simplest form of a vibrating system is the single oscillator with linear components (Fig. 2.1):

$$m\ddot{y} + c\dot{y} + ky = F \quad (2.1)$$

For a system in water,  $F$  represents all hydrodynamic forces. In  $F$  one can sometimes distinguish components which are proportional to  $y$ ,  $\dot{y}$  or  $\ddot{y}$ , in which case a convenient representation of Equation (2.1) is:

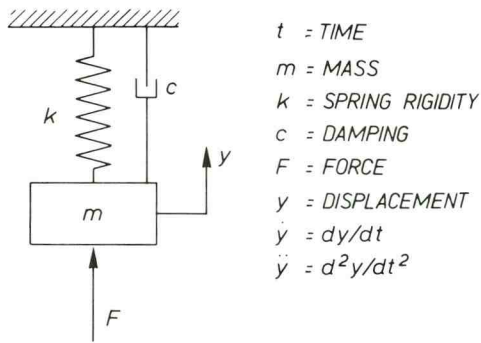


Figure 2.1 The single oscillator; symbols

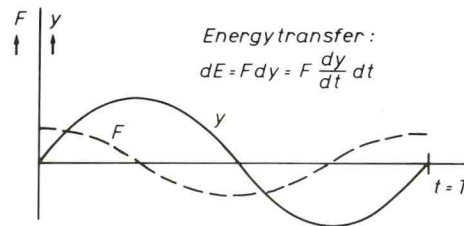


Figure 2.2 Energy transfer between external force and vibrating body

$$(m+m_w) \ddot{y} + (c+c_w) \dot{y} + (k+k_w)y = F_w \quad (2.2)$$

$F_w$  now still contains components which are independent of movement (uncoupled components), but also components coupled with the vibrational movement; only the linear terms have been brought to the left hand side. In Equation (2.2) the factors  $m_w$ ,  $c_w$  and  $k_w$  are the hydrodynamic (or added) mass, damping and rigidity; it is not yet defined whether these hydrodynamic terms are positive or negative.

Whereas the total mass  $(m+m_w)$  and the total rigidity  $(k+k_w)$  together determine the resonance frequency of the system, the factor  $(c+c_w)$  determines whether the system is

- stable (or positively damped) namely when

$$(c+c_w) > 0, \text{ or} \quad (2.3)$$

- unstable (or negatively damped) namely when

$$(c+c_w) < 0 \quad (2.4)$$

In the latter case, self-excitation will take place and one can conclude that the design is wrong. When design criteria are to be defined, the prevention of unstable vibration should be one of the first.

To see if negative hydrodynamic damping can occur, it is convenient to analyse the hydrodynamic forces induced by purely harmonic movement (Fig. 2.2):

$$y = Y_o \sin \omega t \quad (2.5)$$

As long as small vibration velocities  $\dot{y}$  are involved (i.e. small compared to water velocities), one can reason that the hydrodynamic forces coupled to the vibrations are linearly related to  $y$ ,  $\dot{y}$  and  $\ddot{y}$ . So,  $F_w$  will be a harmonic force. When we define

$$F_w = F_1 \sin \omega t + F_2 \cos \omega t \quad (2.6)$$

the energy transferred from the flow to the vibrating body is

$$\begin{aligned}
E &= \int_0^T F_w dy = \int_0^T F_w \dot{y} dt = \\
&= F_1 Y_0 \int_0^T \sin \omega t \cos \omega t dt + F_2 Y_0 \int_0^T \cos^2 \omega t dt
\end{aligned} \tag{2.7}$$

It is obvious that only the second term transmits energy, which means that only a force in phase with the vibrational velocity and working in the same direction will transfer energy. It is demonstrable that this is the case when in Equation (2.2)  $c_w$  is negative.

### Conclusions:

From the general analysis of Equation (2.2), two evident design criteria can be derived:

- Negative hydrodynamic damping should not occur, or must at least be compensated by stronger mechanical damping.
- Dominant excitation frequencies should be well away from resonance frequencies, given by the equation

$$f_r = \frac{1}{2\pi} \sqrt{(k+k_w)/(m+m_w)} \tag{2.8}$$

In the case of flow-induced vibrations, it is the Strouhal number  $S = f L/V$  which is the main descriptive parameter of the excitation frequency ( $f$  = excitation frequency;  $L$  = a representative length of the flow geometry; and  $V$  = a representative flow velocity). When  $V$  is variable, the excitation frequency will also vary; this means that the resonance frequency  $f_r$  must be a factor higher than the excitation frequency  $f$  belonging to the maximum flow velocity. How great this factor should be is still under discussion, but to our opinion one should try to obtain at least a factor 3. In this case, the amplification factor results in an overshoot of 10% above the static deflection, while available data show that there is still no tendency of the excitation frequency to shift towards the resonance frequency.

### 3. CONCLUSIONS FROM THE APPLIED FLUID MECHANICS

The added, or hydrodynamic, mass in its simplest form is represented by a piston in a cylinder partially filled with water (See [1] and Fig. 3.1):

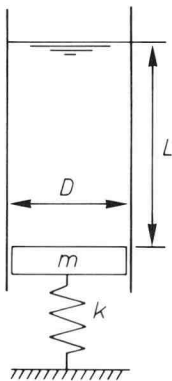


Figure 3.1 Added mass of a piston

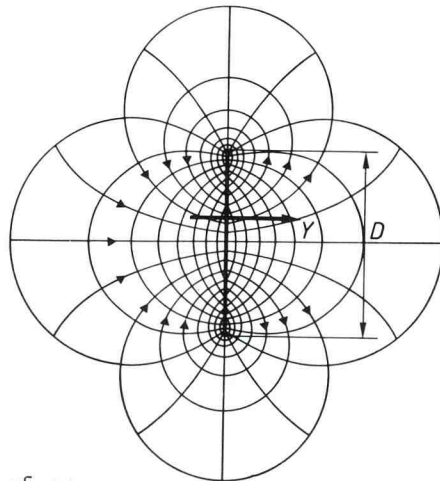


Figure 3.2 Added mass flow of an oscillating strip

$$p = \rho L \ddot{y} \quad (3.1)$$

$$m_w = \rho L \frac{\pi}{4} D^2 \quad (3.2)$$

For vibrating bodies completely submerged in stagnant fluid, Lamb [2] already showed that  $m_w$  can be deduced from potential flow theory and he found an analytical solution for the added mass of slender cylinders of circular and elliptical cross-section, with as limiting case a flat strip (Fig. 3.2):

$$m_w = \rho L \frac{\pi}{4} D^2 \quad (3.3)$$

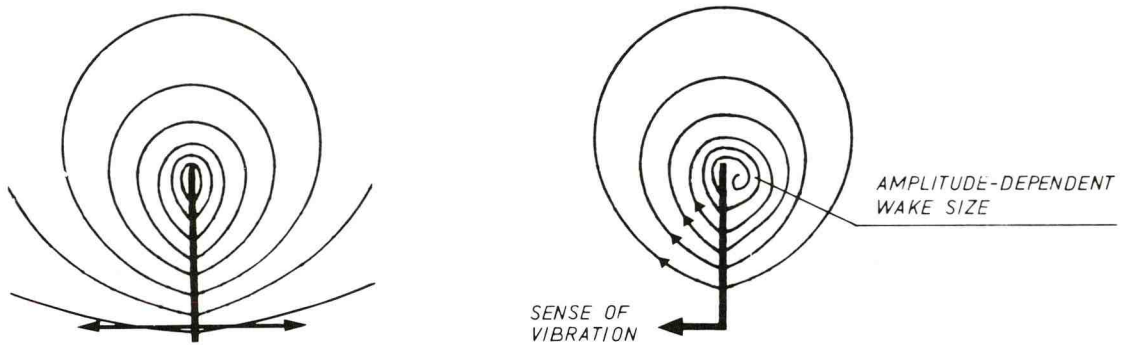


Figure 3.3 Added mass flow without and with flow separation

What is neglected is that flow velocities at sharp edges are infinitely high in potential-flow theory (Fig. 3.3 left), whereas in reality flow separation will appear (Fig. 3.3 right). In stationary flow, flow patterns with separation are considerably different; but in the case of added-mass flow, fluid is sucked around the edge because of a fluid deficiency at the momentary downstream face. Moreover, no vortex street will appear when locally-induced vortices are not transported by the flow.

When the vibrating body is positioned in non-stagnant fluid, the added mass remains unchanged as long as flow velocities are not too great. The determinative parameter is again the Strouhal number  $S = f L/V$ , but now  $f$  is the frequency of the vibrating body.

When, for instance, in the terms of the Navier-Stokes equation for the x-direction

$$\partial p / \partial x = \rho \partial v / \partial t + \rho v_x \partial v_x / \partial x \quad \text{etc.} \quad (3.4)$$

periodic disturbance terms of small amplitude are introduced, the additional terms (indicated by accents) give:

$$\partial p' / \partial x = \underbrace{\rho \partial v' / \partial t}_A + \underbrace{\rho v'_x \partial v_x / \partial x + \rho v_x \partial v'_x / \partial x}_B + \underbrace{\rho v'_x \partial v'_x / \partial x}_{\text{negligible}} \quad (3.5)$$

If  $v'_x$  is proportional to  $\dot{y}$  of the vibrating body,  $\partial v'_x / \partial x$  will be related to  $\dot{y}/L$  (wherein  $L$  is a representative length of the flow geometry) and  $\partial v'_x / \partial t$  is proportional to  $\omega \dot{y}$ .

It can be demonstrated that the B-terms can be neglected as long as the order of magnitude of  $S$  is greater than  $(2\pi)^{-1}$ , and then the velocity  $v$  does not affect  $m_w$ .

Knowing that potential flow problems can be solved with electrical analogues (if the vibration frequency is high enough to neglect wave radiation), or by means of finite-element methods (also applicable when wave radiation is not neg-

ligible), it is possible to determine the added mass for two-dimensional gate vibrations. In an electrical analogue, the free-liquid surface has to be represented by a zero-potential line, as has been shown by Zienkiewicz and Nath [3].

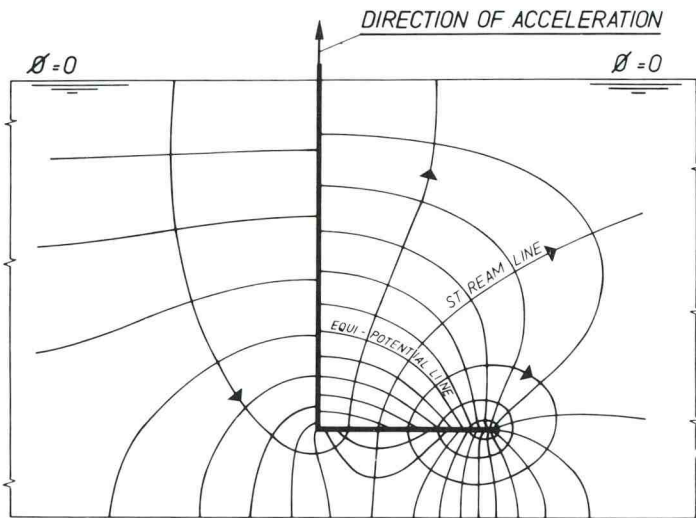


Figure 3.4 Added mass of an L-shaped gate

A solution for a vertically vibrating gate (Fig. 3.4) shows potential differences across the vertical plate; and because potentials represent liquid pressures proportional to the acceleration  $\ddot{y}$ , there are found coupling forces which are due to the added-mass flow (vertical acceleration  $\ddot{y}$  causes a horizontal force).

Figure 3.5 represents in gradual steps how added-mass flow has to be introduced in mechanical systems. It is the third case, which is in general representative of the hydrodynamic mass. This explains why, for instance, vibration modes can differ considerably depending on whether the gate is submerged to a greater or lesser degree in the water.

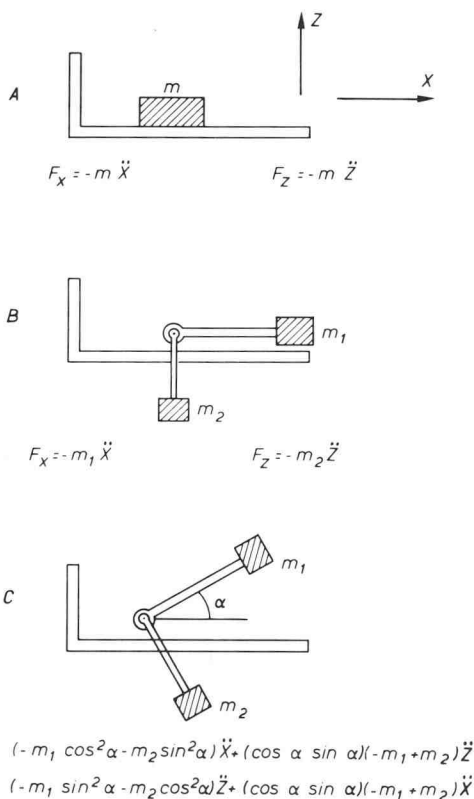


Figure 3.5 Coupling effects of the added mass

When resonance frequencies of a submerged structure are calculated and when the schematization into a lumped mass-spring system with  $n$  degrees of freedom is made, the added-mass effect results in coupling forces wherein the movement of each mass, and this in each of its degrees of freedom, causes resultant pressures on all the masses. The added mass, including the coupling terms, has to be expressed in an  $n \times n$  matrix and can then be introduced into the eigen-value calculations of the lumped-mass system. In [9] this method is introduced for ships and the added-mass matrix calculation is performed by the finite-element method.

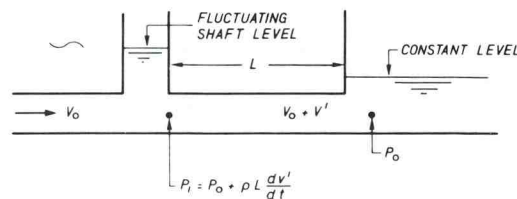


Figure 3.6 Flow inertia in a culvert

Inertia of the water also plays a role under non-stationary flow conditions, namely when the water is accelerated and decelerated. This inertia effect is of a character similar to that of the added-mass flow. The parallel roles of flow inertia and added mass flow in gate vibration can be demonstrated by comparing Figure 3.6 with Figure 3.1.

Inertia of the water in the culvert causes a pressure rise (above  $p_0$ ) in the shaft which is equal to

$$p' = \rho L \frac{\partial v}{\partial t} \quad (3.5)$$

This equation is similar to Equation (3.2).  $L$  can be seen as an "added mass", not of a vibrating body, but the mass of one of the components of an oscillating flow system.

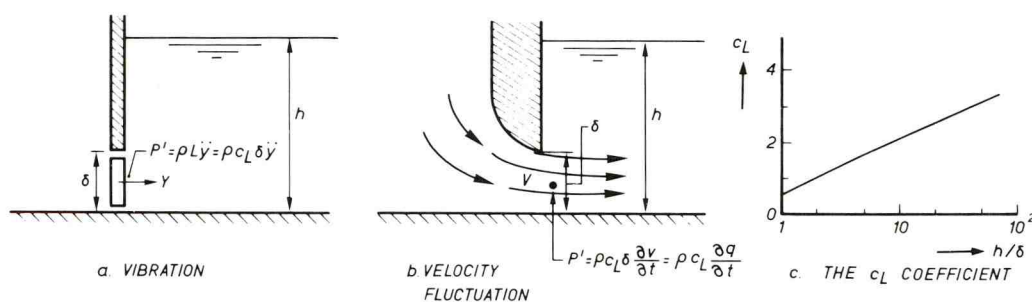


Figure 3.7 Flow inertia at vibrating gate and at fluctuating discharge

In much the same way, there is a parallel in the two cases presented in Figure 3.7: the added mass of a gate and the inertia of a fluctuating flow. The factor  $c_L$ , introduced here, is derived from an imaginary tube with a length  $L = c_L \delta$ , which is assumed to represent the flow inertia.

In the first case, the added mass follows, as explained before, from the potential flow theory. In the second case, this gives only an approximation because

- the velocity  $v$  and its fluctuation  $dv/dt$  are not evenly distributed across the opening and the distribution pattern of  $dv/dt$  is unknown;
- the initial velocity should not be too great: when the velocity fluctuation is periodic, that is when  $v' = \hat{v} \sin \omega t$ , the Strouhal number  $S = (\omega/2\pi) \delta/v$  should, again, not be below a certain minimum value, or else  $c_L$  will be affected.

#### 4. GATE VIBRATIONS EXPERIENCED; PART I

The double-leaf gate of Chart J was rebuilt, making use of favourable experience with the old one over many years. There was a discussion on whether the seal between the two leaves should be asymmetric with a single seal beam, or symmetric with equal beams on both the upper and the lower leaf. The asymmetric seal, with the beam on the lower leaf, was chosen, because this construction relieves the load on the upper leaf when this is lowered (the condition wherein the water pressure would otherwise exert its maximum horizontal load). This solution had already been applied in the old gate, which had functioned correctly during a long period.

After installation of the new gate, strong vibrations occurred. Lowering the upper leaf more than 1.6 m was even unacceptably dangerous. Inspection of the old gate showed that the paint had been scratched over the entire overlap area. So, there had been no leak gap! Putting a plastic rain pipe on top of the lower leaf to seal the leak gap immediately stopped the vibrations. A similar permanent so-



lution was then applied (Sketch 3 of Chart J).

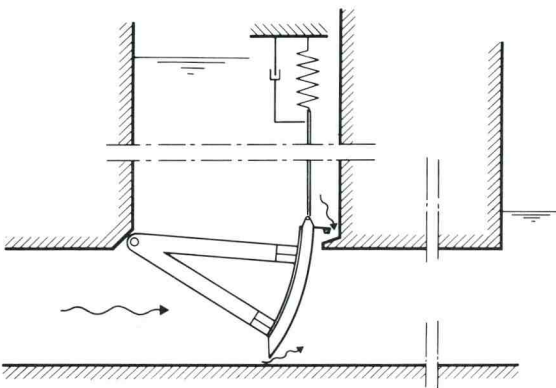


Figure 4.1 Vibration of reverse Tainter valve due to protruding lip

The reversed Tainter valve of Figure 4.1 (see also Chart C) had to be free of vibration and was therefore designed with a sharp lower edge. In the bottom of the culvert, a strip of hard rubber was installed to provide a tight seal. Wear of this bottom rubber and the resulting change of position of the closed gate demanded a softer, slidable top seal. Therefore, a top seal was proposed with a protruding beam (solution A), which was tested in the existing hydraulic model. At small openings, the tests showed very strong vibrations, with hoist forces of 1.5 to 2 times the weight of the gate; sometimes these vibrations were only limited because the gate hit the bottom.

The solution decided on (sol. B) was based on two principles:

- reduction of the upper gate lip, and
- reduction of the clearance between the gate and the shaft wall by means of a protruding steel plate to prevent pressure pulsations in the downstream culvert acting on the lip.

The principle of this solution was probably first published by Petrikat.

After all, a further improvement might have been found in a rubber profile clamped along both edges (sol. C of Chart C), as there still can be heard a weak vibration in the actual gate during a (very short) period after the gate has begun to rise. This probably occurs in the range where the initial gap is narrower than, or of the same order as, the gap between the skin plate of the gate and the protruding plate in the shaft.

Chart K presents a vertical-lift culvert gate for a navigation lock between a salt-water and a fresh-water basin wherein leakage has to be fully prevented in closed condition. This demand led to a gate with a circumferential seal on its downstream face, sealing against a seat recessed in the wall of the culvert. To prevent seal damage during movement of the gate, the gate was released from its seat by means of cranked wheel axles coupled to the hoisting bars.

In a hydraulic model, horizontal vibrations should be studied by providing the gate, instead of wheels, with four arms projecting outside the culvert and supported on vertical leaf springs which allowed horizontal and torsional gate vibrations (Fig. 4.2). It became apparent in the model that a strong horizontal vibration of the gate began the moment it came free from its seat, and stopped when the release distance was increased. The frequency of the gate/spring oscillator decreased when the gap was small, as hindrance of added-mass currents around the gate edges caused an important part of the culvert water mass to act as added mass.

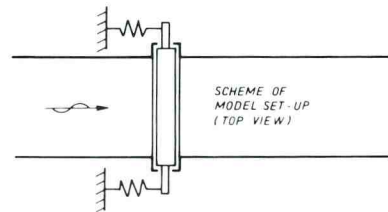


Figure 4.2  
Scheme of model setup for horizontal vibration study of vertical-lift culvert gate

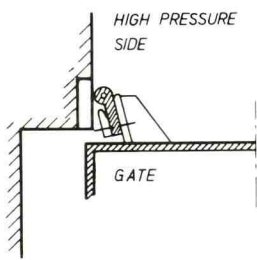


Figure 4.3 Music note seal and flap seal

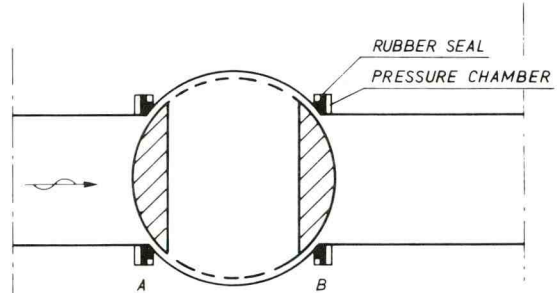


Figure 4.4 Inflatable seal of ball valve

In all cases where an elastical seal (e.g. a music note seal) is tightened by the water pressure, a small leak gap can cause strong vibrations (Fig. 4.3). Such a seal was applied at a mitre gate in a medium-head navigation lock wherein a leak gap had developed due to damage caused, it was suggested, by a floating log that had deformed the seal. When the gate was under its full head of 8 m, no vibrations occurred; but at heads between 2 m and 6 m, vibration of the entire gate became so strong that extra damage to the gate pivots was suspected to be imminent.

At the lower end of a penstock of 500 m head, carrying water to a Pelton turbine, a ball-type shut-off valve and a needle-type regulating valve were provided. When the ball valve (Fig. 4.4) was closed, but the seals not yet inflated, a strong vibration developed with a period of 3 seconds and pressure pulses which damaged the seal operation system. The vibration period corresponded with the basic period of the standing waves that could occur in the penstock. A similar case is described by Streeter and Wylie [4], wherein water hammer calculations revealed that the water column/valve system could become unstable when the valve characteristics showed a decrease of discharge capacity caused by an increasing pressure head. This condition is a possibility when an elastical seal has a tendency to be closed by an increasing pressure, like for instance the music note seal described above.

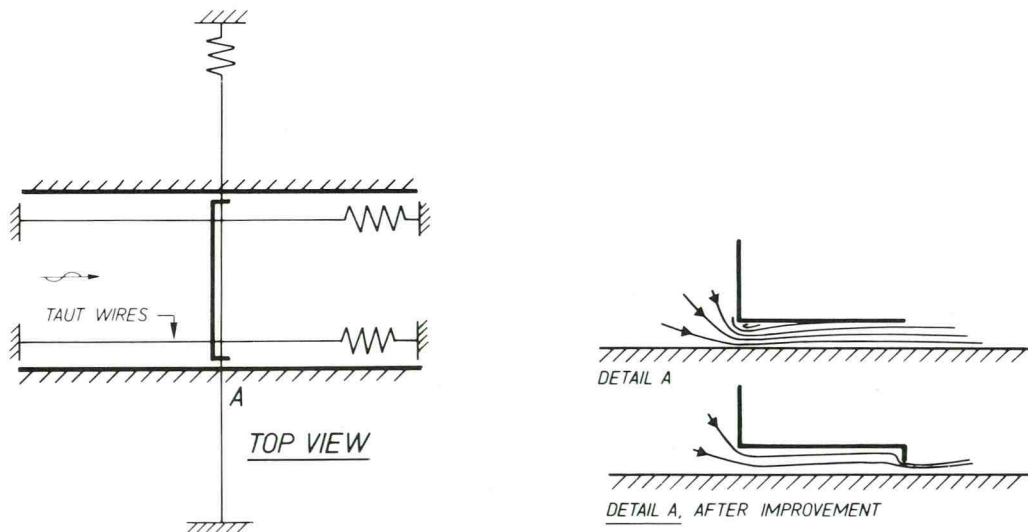


Figure 4.5 Top view of model for studying vertical vibration, but which vibrated transversely

Figure 4.5 shows a hydraulic section model of an underflow-type gate; side leakage was accepted between gate and flume wall to permit frictionless vertical gate vibration. The gate was stabilized by a series of horizontal wires, attached at two levels (above the water) so as to permit only vertical vibration of the gate. It was suspended by a vertical wire from a leaf spring of adjustable rigidity. To our surprise the gate started to vibrate in transverse direction and, due to the relatively high rigidity in the horizontal wires, quite high frequencies of 10-15 c/s were involved. The depth of the water at the downstream side was on the average 30 cm and the head difference varied between 10 and 45 cm. The leak gap was about 4 mm. The remedy was found in decreasing the gap locally to 2 mm. The narrow part had to be at the downstream end of the gap to be effective.

During preliminary investigation of an underflow gate with 30 m span, a section model was built to see if it would be acceptable to protect the girders from wave attack by a second vertical plate. The horizontal girders were designed as an open frame; see further Chart A. The model was only suited to investigate vertical vibrations and had hardly any structural damping. In a later stage, when decisions about the general shape of the gate had been made, a three-dimensional elastic model was planned for an overall check of the design.

The investigation in the two-dimensional model revealed that condition  $T_0$  (see Sketch 3 of Chart A) showed a critical gate position in which the (single) amplitude of the hoist force became about 25% of the gate weight.

The model showed that a stable gate design could be arrived at (except for very small openings, which were not further investigated at that moment) on the condition that the upstream gate lip was the one with the bottom seal. A further improvement could be obtained by extension of the upstream gate lip.

As further presented in Chart B, the same gate was subsequently reproduced in an elastic model (scale 1:25) to check the results of the first model and to establish the optimum seal shape for the prevention of vibrations at small openings (for details see Sketches 3 and 4 of Chart B). A problem with this model was that it was impossible to reproduce wheel friction. Although this friction was not very high, it hindered reproducibility in the vertical vibration tests. For these reasons the model gate supplied with wheels was not suited to study vertical vibrations, so a part of the tests were done with the gate supported by horizontal leaf springs which allowed it to move only vertically and without friction. In other tests wheels were used, while force meters between the wheels and the gate measured the horizontal vibration forces.

Various types of vibration arose in the model. Vibrations occurred at gate openings of the order of the seal width, independent of the value thereof. These vibrations were hardly acceptable; because of variable gate flexure due to tidal action, the provision of a leak gap at closed gate position was proposed. These vibrations occurred only in the setup for vertical vibration at head differences greater than 3 m prototype value.

After initial vertical vibration, horizontal vibration became dominant. During vertical vibration, waves radiated away from the gate in the upstream basin (Fig. 4.6a), whereas horizontal vibration resulted in a pattern of intersecting waves generated mainly at the corners (Fig. 4.6b). Vibration stopped when the gate was touched with the hand at the abutments and also stopped when the leak flow in the recesses was reduced to nearly zero; a gap of less than 75 mm prototype value did already reduce the intensity.

The older gate of Chart L is the downstream gate of a 5 m head difference navigation lock. Problems arose after a revision in which, among other things, the wooden seal beam was replaced by a new one. At lifts between 0.13 and 0.35 m, the 14 m span wheel gate became subject to strong horizontal vibration of about

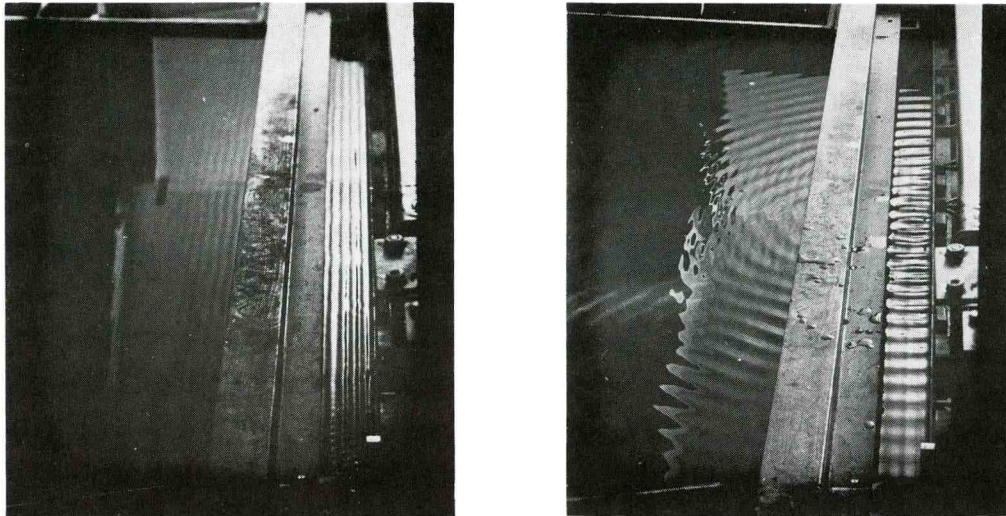


Figure 4.6 Wave radiation upstream at vertical and at horizontal gate vibration (Volkerak sluice gate; see Chart B)

5 c/s and 5 mm amplitude (single). It started with vertical vibration of much smaller amplitude, whereupon horizontal vibration became dominant, generating a pattern of intersecting waves (Photo in Chart L).

A remedy for the vibrations was found in the provision of 1 m spaced, 0.4 m long pieces of steel angle bar as disturbance elements along the upstream side of the seal beam in order to prevent a complete synchronization of the vortex street. For further data see Chart L.

#### Conclusions:

- All the above vibrations occurred (or started) in the direction wherein the flow gap width or the leakage fluctuated due to the vibration.
- The excitation mechanism appeared to be strong and was probably much stronger than can be explained by local vortex shedding. It seems justified to say that the resulting discharge fluctuations - due to the inertia of the upstream and downstream water - give rise to pressure fluctuations which act on the gate even in zones remote from the seal. This explanation is confirmed by a recent publication of Miller of the Hydraulic Institute at Stuttgart [5], showing that pressure measurements at the skin plate of a gate at different distances from the gap revealed amplitudes that decreased with the distance; but no phase shift occurred.
- In all the examples it can be seen that - when one assumes a constant discharge - the buildup of pressure when the gap narrows results in forces on the gate and the seal in a direction tending to a further decrease of the gap (a sort of negative hydrodynamic rigidity). This empirical conclusion has long been used in the Delft Hydraulics Laboratory as an instability indicator [8]. Sometimes the pressure acts directly; sometimes indirectly, namely when a narrower gap results in an extra head difference, which results again in suction forces at the gate edge.
- The use of the instability indicator reveals that those gates where stationary suction forces do occur (forces tending to decrease the gap) are sensitive to vibration.

#### 5. FLOW BEHAVIOUR WHEN THE GAP WIDTH FLUCTUATES

To illustrate flow phenomena that are related to vibrations due to fluctuating gap width, elements from my lecture held at Baden-Baden will be used [1]

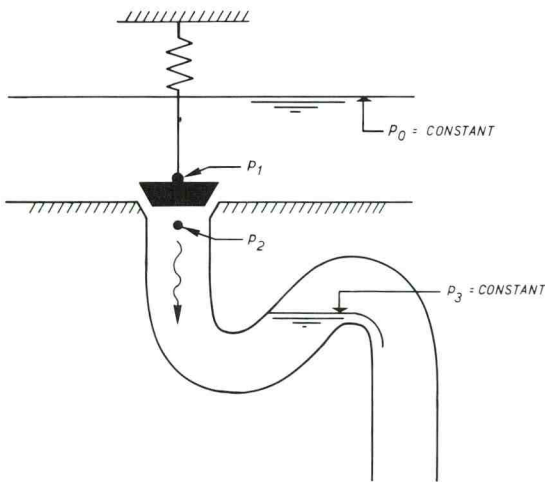


Figure 5.1 The vibrating bath-tub plug

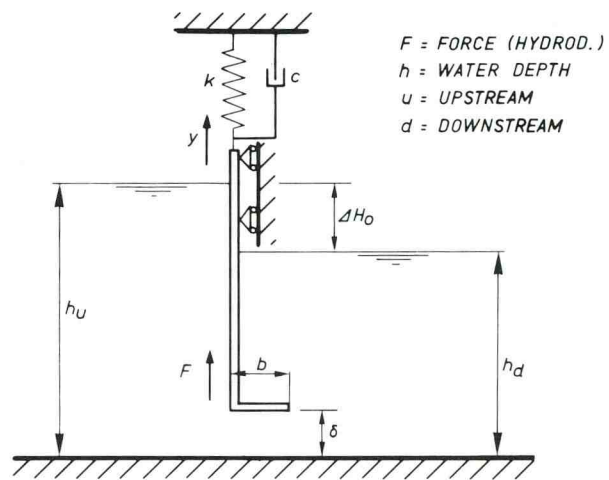


Figure 5.2 Scheme of vertically vibrating gate

The bath-tub plug of Figure 5.1 is a good illustration, because everyone knows from experience that when one closes the drain while the bath is emptying, a great force is felt to be exercised on the plug during the final closing motion. In a way, the plug is sucked in by the flow and, apparently, the inertia of the water in the drain pipe makes it difficult to stop the discharge immediately. Moreover, holding the plug so as to leave a very small opening always leads to a shaking movement of the plug.

We shall now examine what forces are induced by the water during harmonic plug vibration, and then analyse if there are forces in phase with the vibration velocity, which are indicative of self-excitation.

At low frequencies, the discharge will follow the momentary discharge capacity, which is related to the gap size: an upward plug movement  $y$  causes an extra discharge  $Q'$  (appr.  $Q' \propto y$ ). The pressure difference ( $p_2 - p_3$ ) over the length of the pipe is related to  $\partial Q / \partial t$  of the pipe flow, and, because  $p_3$  is constant,  $p_2$  increases proportionally to  $Q'$  and also proportionally to  $\dot{y}$ ; this causes self-excitation (see Par. 2).

At high frequencies, the discharge remains constant due to pipe flow inertia. When, for instance, the gap increases by a value  $y$ , the head difference across the gap will decrease; this means that a negative hydrodynamic rigidity is found and the negative hydrodynamic damping is gone. So the hydrodynamic forces get a  $90^\circ$  phase shift compared to the low-frequency condition (this conclusion will be used in Par. 7), and it can be concluded that an increase of the vibration frequency (increase of rigidity) is a measure which will decrease negative hydrodynamic damping.

A similar mechanism can be found in the case of vertical vibration of an underflow gate (Fig. 5.2) when one assumes that the seal shape is such that a suction force is generated proportional to the local head difference across the gate. In the upstream and downstream water there will be inertia effects, such that an increase of discharge (under the gate) per unit of time ( $\partial Q' / \partial t > 0$ ) causes a decrease of pressure upstream and an increase downstream. (One can, for example, use Fig. 3.7 to find the order of magnitude.) This means that with a positive value of  $\partial Q' / \partial t$  there is a proportional decrease of head difference

across the gate. Now a similar line of reasoning can be followed as was given for the bath-tub plug.

At low frequencies, when  $y$  is positive, again  $Q'$  becomes positive. The local head difference decreases proportionally to  $\dot{Q}'$  and proportionally to  $\dot{y}$ , and the related suction force will also decrease proportionally to  $\dot{y}$ . This again, as in Paragraph 2, indicates self-excitation.

At high frequencies, when  $y$  is positive, and now assuming that  $Q$  remains constant due to the inertia of the flow, the gap height increases and, together with the constant discharge, the head difference across the gate will decrease, as will the suction force. Now the harmonic force is in phase with  $y$  and there is a negative hydrodynamic rigidity.

This theory has been evaluated quantitatively, and Figure 5.3 shows the ranges of the Strouhal number where self-excitation and where negative hydrodynamic rigidity can occur. The contraction coefficient  $\mu$  depends on the seal shape, while the inertia coefficient  $c_i$  is obtained by adding the imaginary tube lengths upstream and downstream (to be found with the aid of Fig. 3.7) and the seal width. For practical purposes  $c_i$  varies between 4 and 10 for free-surface flow gates. Experimental verifications of the theory [6] showed a sensitive region, as indicated in Figure 5.3. This corresponds to a Strouhal number  $S_\delta = \frac{f \delta}{\sqrt{2g \Delta H}}$  in the range of 0.025 to 0.1 (see the maximum of the "experiment" curve in Fig. 5.3 obtained with  $\mu = 0.6$  and with  $c_i$  varying between 4 and 10).

Note that gate vibrations at a rectangular seal do not only occur at smaller gate openings, where reattachment of the flow against the seal causes a suction force. At openings where reattachment is absent, however, vibrations are weaker. A theoretical explanation of this phenomenon is also presented in [6]; it defines an imaginary suction caused by flow inertia in the downstream water only.

#### Conclusions:

From the foregoing one may deduce the so-called fluctuating-gap theory.

- The occurrence of a negative hydrodynamic rigidity at high frequencies coincides with the occurrence of self-excitation at low frequencies; this is the theoretical base of the use of the instability indicator.
- The instability indicator can also be used in a second way: when a slow closing of the gap is considered, the inertia of the water creates regions with an increase and with a decrease of pressure; when the resultant force on the gate is in closing direction, negative hydrodynamic damping occurs.
- The use of the indicator reveals that stationary suction forces (tending to close the gap) result in a tendency towards self-excitation.
- Extra safety against this type of vibration is obtained by increasing the rigidity of the gate so as to increase the resonance frequency, and consequently the  $S_\delta$ -value; the theoretical damping curve of Figure 5.3 illustrates the decrease of self-excitation.
- For vertical vibrations rather low critical  $S_\delta$ -values are found: between 0.25 and 0.1.
- From Figure 5.4 one can see that horizontal as well as vertical vibration can induce discharge variations. When, due to flow inertia in the culvert, these discharge variations, in their turn, cause pressure variations downstream of the gate, horizontal and vertical forces are induced. This is, in addition to the coupling by added-mass flow, the second coupling phenomenon of various vibration modes.

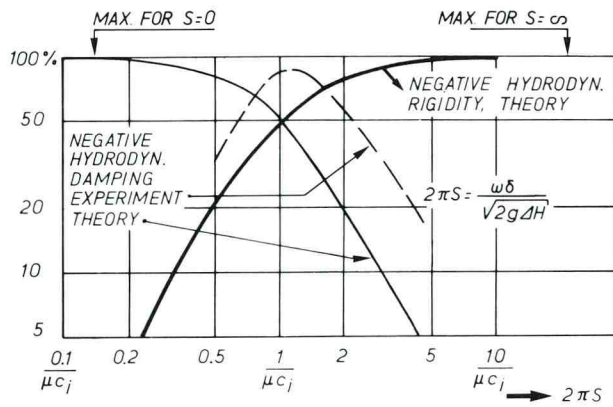


Figure 5.3 Negative hydrodynamic elasticity and damping of rectangular shaped gate (or gate lip) as function of Strouhal number

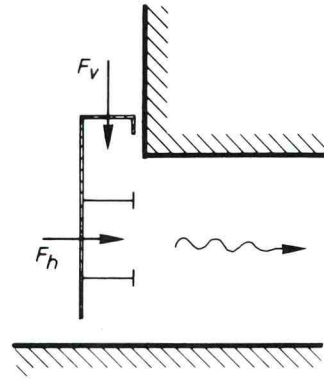


Figure 5.4 Situation where coupling effects between horizontal and vertical vibration may occur

## 6. GATE VIBRATIONS EXPERIENCED; PART II

The visor gates of the Lower Rhine canalization in the Netherlands (see also Chart G) have already functioned for more than 15 years now. They have been used to check elastic similarity models; models which reproduce the lower-frequency vibration modes, but not local high-frequency plate vibrations.

The design of their lower edge (Sketch 3 of Chart G) was based on the argument that, in closed position, the gates would be adequately supported by the fender profile extending along their length and that, when partly raised, no adverse effects had been found at the four lower resonant vibration modes (up to about 6 c/s) in the hydro-elastic models. Theoretically, a negative aspect of the fender profile is that at a semicircular profile the flow separation point is not well defined and may be largely influenced by a small disturbance.

After construction, high-frequency plate vibrations occurred at the corners of the gate when the local gate lift there was of the order of 0.5 m. Strengthening and stiffening of the plates led to only partial success. The vibrations have now been accepted, though in critical circumstances a remedy is available in the form of an added lift of one gate and a reduced lift of the other, thus maintaining the same total discharge capacity.

In a hydraulic model, we intended to perform pressure measurements with an unfavourably shaped quarter-elliptical gate seal (Chart M). A 2 cm steel plate was wedged between the flume walls. The construction was strong and stiff enough for a maximum head difference of 50 cm water. Nevertheless, horizontal plate vibration became apparent, generating a cross-pattern of waves in the upstream water. Frequencies were not measured; analysis of the wave pattern (with  $\lambda \approx 2$  cm) shown in the photograph of Chart M indicated a frequency of about 11 c/s, but personal impressions (from the rumbling noise) pointed to about 20 c/s, which frequency agreed with the calculated value of the first natural frequency of the submerged plate.

Chart D shows an emergency flap gate, arranged to lie down flat in normal circumstances. These gates are to provide safety, should a dike rupture locally, by preventing the entire canal system to empty through the gap. During closing movement, flow can occur in two directions; let us call them normal flow (as shown in Sketch 1 of Chart D) and reverse flow. To prevent nappe vibration during normal flow, the gate top had to have higher and lower sections of 2 m length,

because splitter plates were not allowed, as ship's anchors might get fouled therein. For reverse flow, precautions had to be taken, such as a row of spaced blocks under the edge (found in Chart D), to keep the flow attached in all gate positions in order to prevent vibration.

During verification tests with normal flow in the hydraulic model, extremely heavy vibration occurred when the nappe was relatively thick and the air under the nappe was sucked off. This was one of the very few examples of gate vibration in a model, wherein increased hoist rigidity had an adverse effect. A little aeration was sufficient to suppress the vibration. It was decided to install two splitter plates near the abutments. In this case, the great distance between the splitter plates (30 m) was considered acceptable, which, by the way, is not the case when they serve to prevent nappe oscillation. For further details of the conditions wherein vibrations occurred, see Chart D.

### Conclusions:

Three empirical conclusions can be drawn from the foregoing:

- Edges at which unstable flow separation might occur cause danger of vibration, even vibration in the direction in which the gap size remains constant. Such vibrations can also occur when the gate lift is a few times greater than the seal width.
- These vibrations tend to have relatively high frequencies; the Strouhal numbers of the examples were:  
 $S_{\delta} = f \delta / (2g \Delta H)^{1/2}$  of the order of 0.5 - 2 ( $\delta$  = gate opening),  
 $S_b = f b / (2g \Delta H)^{1/2}$  of the order of 0.2 - 1 ( $b$  = width of seal beam).
- In conditions with an overflow nappe where the air underneath can be sucked off by the nappe, resulting in a low-pressure zone, aeration should be applied.

### 7. FLOW CONTRACTION FLUCTUATIONS

The vibrations mentioned in Paragraph 6 were all in a direction in which the gap width or nappe thickness were not, at first impression, varied by gate vibration. Flow and force analysis, assuming a constant discharge coefficient of the gap flow, leads to the conclusion that only damping occurs; the gate acts in the same way as does a body in flow which vibrates in the flow direction.

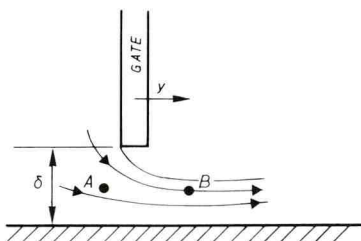


Figure 7.1 Calculation scheme for horizontal vibration (with constant discharge coefficient)

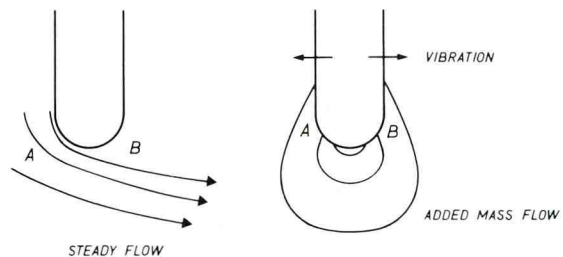


Figure 7.2 The elements of simultaneously occurring gap flow and added-mass flow

The detailed computation, presented in [8], is based on the following principles (see also Fig. 7.1):

- A horizontal gate oscillation is assumed; the displacement is  $y$ .
- A fluctuating additional discharge  $q'$  is assumed, which is superposed on the initial discharge  $q_0$ .
- Both gate vibration (related to added mass flow) and discharge fluctuation (related to flow inertia) cause an extra head difference across the gate



$(\Delta H_{\text{gate}})$  and across the gap  $(\Delta H'_{\text{gap}})$ .

One can now express the equalities:

$$\Delta p'_{AB} = \rho g \Delta H'_{\text{gap}} = -c_L \rho \frac{\partial q}{\partial t} - c_{\text{gate}} \rho \delta \frac{\partial^2 y}{\partial t^2} \quad (7.1)$$

(points A and B are indicated in Fig. 7.1;  $c_L$  is related to  $c_L$  in Fig. 3.7), and

$$\rho g \Delta H'_{\text{gate}} = -c'_L \rho \frac{\partial q}{\partial t} - c'_{\text{gate}} \rho \delta \frac{\partial^2 y}{\partial t^2} \quad (7.2)$$

The discharge equation

$$q_0 + q' = \mu \delta_0 \sqrt{2g(\Delta H_0 + \Delta H'_{\text{gap}})} \quad (7.3)$$

relates  $q'$  to  $\Delta H'_{\text{gap}}$ .

Of the four variables  $\Delta H'_{\text{gap}}$ ,  $\Delta H'_{\text{gate}}$ ,  $q'$  and  $y$ , one can, by using these three equations, find a relation between  $\Delta H'_{\text{gate}}$  and  $y$ ; and one can also find the phase difference. This results in an added-mass effect and a (high) damping term, but there is no self-excitation. This analysis is presented in Reference [8], Chapter 4.

When one has to assume that the flow contraction coefficient fluctuates during vibration, a possible explanation is that the added-mass flow - i.e. the flow wherein the velocities vary in phase with the vibration velocity of the gate edge.- can have an effect on the flow contraction, especially, but not exclusively, in the case where a rounded edge already induces a very sensitive flow pattern (Fig. 7.2). This effect would operate in such a way that edge movement in the  $y$ -direction (to the right) causes a flow around the edge which tends to decrease the discharge coefficient.

When the contraction coefficient is also expressed in a constant part  $\mu_0$  and a fluctuating part  $\mu'$ , it is of interest to know if  $\mu'$  varies proportionally to the vibration displacement  $-y$ , to the vibration velocity  $-\dot{y}$ , or to the pressure gradient (related to  $-\ddot{y}$ ). If the vibration is entirely parallel to the bottom, the relation of  $\mu'$  to  $-y$  is improbable. There remain:

possibility a: the flow is sucked around the edge by the right-hand part of the added-mass flow ( $\mu'::-\dot{y}$ ); and

possibility b: the boundary layer becomes unstable (early flow separation) when there is a positive pressure gradient in the flow direction ( $\mu'::-\ddot{y}$ ).

Similar reasoning as used in the gap-flow theory of Paragraph 5 leads to two possibilities: low-frequency and high-frequency vibration.

At low frequency, the discharge fluctuates proportionally to and in phase with  $\mu'$ , resulting in a pressure difference across the gate and the gap proportional to  $-\partial q'/\partial t$ , due to the inertia of the up- and downstream water.

At high frequency, the discharge remains constant due to flow inertia, and in this case the head across gate and gap varies proportionally to  $-\mu'$ .

Between these two cases there is again a  $90^\circ$  phase shift of the forces involved. In the fluctuating-gap theory, this results in negative hydrodynamic damping for low-frequency vibration and negative hydrodynamic rigidity for high-frequency vibration (Par. 5). Qualitative analysis of the phase shift between the head difference across the gate and the vibration displacement  $y$  reveals that negative hydrodynamic damping ( $\Delta H'::\dot{y}$ ) occurs only at a combination of possibility a and high-frequency vibration.

That this combination indeed leads to self-excitation can be explained in the following way:

When at high-frequency vibration, where the discharge remains constant, a smaller

value of  $\mu$  results in a greater head difference across the gate ( $\Delta H' = -\mu'$ ) and also  $\mu = -\dot{y}$  (possibility a), the head difference is in phase with and in the direction of the vibration velocity. These conditions being fulfilled, negative hydrodynamic damping will occur (when other components do not give too high a positive damping).

In the case of the flap gate with overflow (Chart D), the flow is probably stably attached at the upstream rounding of the crest. But at the moment when vibration lowers the gate, the added-mass flow will tend to influence the nappe path such that the water will fall farther away. This, however, is prevented by the constant volume of water under the nappe, resulting in a low pressure in phase with the vibration velocity.

## 8. GATE VIBRATIONS EXPERIENCED; PART III

In the same series of experiments wherein the quarter-elliptical gate seal was tested (Chart M), a rectangularly shaped gate edge was tested for suction forces, using a rigid model. The gate, including the edge, was again the 2 cm thick steel plate, wedged between the walls of a flume (Chart M). High-frequency bending vibration was observed (15-20 c/s) at gate lifts of 1.35 and 2 cm, but not at the other lifts of 1, 3 and 14 cm. The head differences were 0.2-0.4 m. Especially at a lift of 1.35 cm (and  $\Delta H = 0.4$  m), vibration was intense.

There is a tendency in the Netherlands to suppress seal beams and make sharp-edged gate lips whenever watertight closure is not needed. This holds particularly for storm-surge barriers, where the varying load at closed position can cause wear of the seals. However, problems can arise.

The 80 m span gate at Krimpen (Chart H) was tested at head differences of up to 2 m. Only in "closed" position, when a minimum gap width of officially 3.5 cm is available, a high-frequency plate vibration was felt. Above water (depth about 7 m), a spectrum of vibration frequencies was measured, with a clear peak at 88 c/s, which corresponds roughly to the natural frequency of the gate lip. When the gate was raised only a little, the vibration stopped.

In a complex of restored antique navigation locks (the Great Sea Locks at Muiden, near Amsterdam), one of the locks was adapted for sluicing. To hide the sluicing gates from sight, a steel frame with two butterfly gates was mounted under a bridge (Chart E). Here also, a leak gap at closed gate position was designed, and the gate plate (with reinforcement ribs at 65 cm intervals) ended with a sharp edge. In a 1:10 model, the rigidity was reproduced (but not the plate mass, because the added water mass was considered to be predominant). So, the plate thickness of the model was 1.25 cm (prototype value) instead of 2 cm. With a leak gap of 1 cm, strong plate vibration was felt between closed gate position ( $\phi = 0^\circ$ ) and  $\phi = 3^\circ$ , and the torque meter at the central gate shaft indicated a frequency of 50 c/s (prototype value).

A remedy was found in mounting seats on the jambs of the surrounding frame, against which the plate was pressed in closed position. Moreover, the plate edge was stiffened; and the jamb edges were bevelled in order to obtain a rapid increase of the gap width at initial opening of the gate without causing a complete change of direction of the water jet. Further details can be found in Chart E.

Chart B was already presented in Paragraph 4; the thickness of the lower edge of the 1:25 elastic similarity model of the Volkerak gates (span 30 m) was varied in order to study the suppression of gate vibration at small openings, that is, at closed position of the gate. Whenever the gate lift was between 0.7 and 2 times the width of the gate edge, vibration occurred, always starting as vertical vibration (2.9 - 3.6 c/s prototype value), but continuing as horizontal vibration (2 - 2.5 c/s) mainly of gate-bending type. The advice was to make the

edge sharp and to maintain a gap of a few cm in closed position of the gate.

Conclusions:

- Rectangular-section gate seals do not only induce vibration in the direction in which the gap width varies, but also in other directions.
- For a gap between a rectangular gate edge and a flat bottom, the most critical ratio between gap width and gate width is 0.7 - 2.
- Frequencies are relatively high; most of them correspond to a Strouhal number of  $S_b = f b / \sqrt{2g \Delta H} = 0.1 - 0.25$ .

9. GATE VIBRATIONS EXPERIENCED; PART IV

The butterfly gate of the restored old navigation locks with butterfly sluicing gates (Chart E) showed the same high-frequency plate vibration of about 50 c/s (prototype value) at gate opening angles of about  $\phi = 50^\circ$ . This angle corresponds roughly to the gate position at which local flow separation becomes complete flow separation at the downstream side; this can be concluded from the stationary torque measurements.

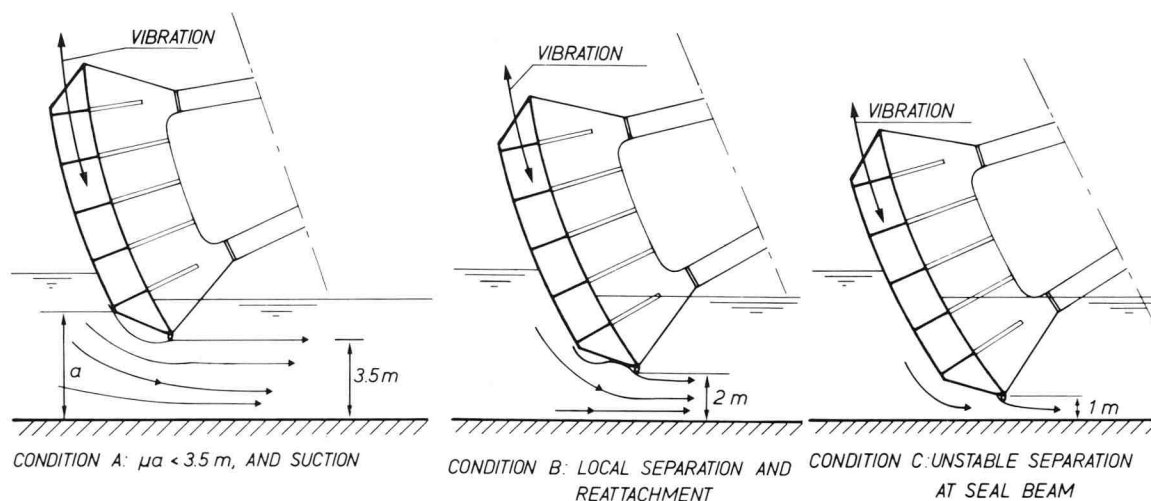


Figure 9.1 Tangential vibrations of sector gates of Haringvliet sluices; elements of flow pattern which can cause vibrations at different gate positions (Chart F)

Figure 9.1 shows the Haringvliet sluices, controlling the discharge of Rhine water into the sea and closing off a fresh-water reservoir; they comprise a double row of sector gates, hinged to the seaside and to the landside of a bridge (see also Chart F). The landside gates have their cylindrically curved plate, and the seal, at the seaside to prevent tangential force components due to wave action.

At the time model studies on vibration were executed, attention was concentrated on the shape of the seal and therefore only gate lifts of up to 1 m were studied. In the prototype, however, vertical (or better: tangential) vibrations occurred at gate lifts of 1 - 4.5 m. The 500 ton gates with a span of about 60 m came into a regular vibration with a maximum (single) amplitude of 2 mm and a frequency of about 2.5 c/s. It must be remarked that, due to the inflatable side seals, mechanical damping at raised gate position is extremely low.

It is only at higher gate positions (condition A) that one can explain such vibrations with the fluctuating-gap theory, or that one can use the instability indicator in the following way: a lowering of the gate at constant discharge causes extra suction, because this suction is related to the increased head dif-

ference across the gate. (When the jet touches the seal, the contracted flow has already expanded again so that near the contraction zone there is a low-pressure zone with underpressures proportional to the head difference.)

At lower gate positions (condition C), a lowering of the gate at constant discharge causes, to the contrary, an increased pressure under the gate, because the gate edge, which regulates discharge, is situated at the downstream side of the gap. Near the upstream side there is a suction zone, but because of the wider flow section there, water velocities increase only slightly and therefore lowering of the gate does hardly create an extra suction force there either.

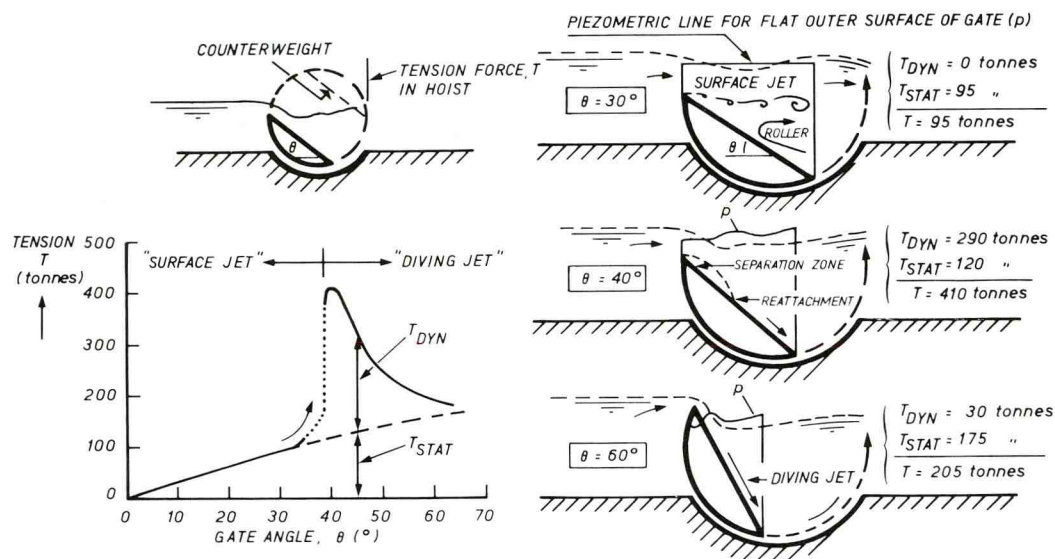


Figure 9.2 Tangential vibration of Thames Barrier gate; instability of flow reattachment (Ref. [7])

The example of Figure 9.2 is included in this paper, although it is not from the Delft Hydraulics Laboratory but from the Imperial College in London. Dr. Hardwick showed me a small section model of the Thames Barrier and he demonstrated that, in conditions wherein the flow wavered between full flow separation and reattachment, vertical (or better: tangential) vibrations occurred. In his paper [7], from which he kindly permitted me to use Figure 9.2, he also demonstrated that by perforating the gate in the low-pressure zone vibrations were reduced. After all, this remedy was not necessary, because in reality the gate frequency was outside the frequency range of these self-exciting vibrations.

Conclusions: The examples of this series have in common that a local low-pressure zone between flow separation and reattachment is involved and reattachment is unstable.

#### 10. CONSIDERATIONS ABOUT FLOW SEPARATION AND REATTACHMENT

In Paragraph 7 it has been suggested that the added-mass flow could influence the point of flow separation at a rounded edge, where the point of separation is unstable and undefined. It is conceivable that the same mechanism could, in the case of a stable point of separation, influence the flow contraction directly, but to a lesser degree. As yet, however, no vibrations have been attributable to such a case (except for the case with an overflow nappe discussed in Par. 7); the rectangular edge of Chart M did not vibrate at wider openings than the seal width. But vibrations can occur when there is a stable flow separation point followed by

reattachment, especially when reattachment of the jet is uncertain. These two conditions, full separation and reattachment, make a considerable difference in the discharge coefficient.

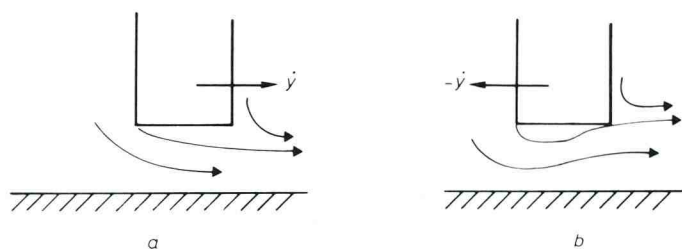


Figure 10.1 Flow pattern at vibration stages with vibration velocity in flow and counter-flow direction

When we consider (Fig. 10.1) a high-frequency horizontal plate vibration wherein  $Q = \text{constant}$  (due to the high frequency) and the velocity =  $-\dot{y}$  (directed to the left), the jet will be sucked upwards by the added-mass flow and reattachment is possible. This increases the discharge coefficient considerably, while the head difference across the gate will decrease accordingly, causing a force in phase with  $\dot{y}$ . With this mechanism all examples of Paragraph 8 can be explained.

When, downstream of the edge, the flow wavers between remaining attached to the face plate of the gate and getting separated, the added-mass flow can also have substantial effects. This is the case with the butterfly gates in the old navigation locks at Muiden (Chart E) and also with the gates in the Thames Barrier (Sketch 4 of Chart E and Fig. 9.2).

The vertical gate vibrations at the Haringvliet sluices (Fig. 9.1) form a special case, but here too the same line of reasoning can be followed. Due to the cylindrical curvature of the skin plates, vertical (tangential) gate vibrations only cause an added-mass flow by displacing water underneath the gate (like a heaving ship). The added-mass flow is more or less symmetric, and the flow contraction and the point of reattachment of the continuous flow are both affected. During downward movement, the contraction coefficient decreases, but at the same time the local low-pressure zone between the points of flow separation and reattachment increases in size, and consequently extra suction is created. Because this suction now again is in phase with the vibration velocity, self-excitation can occur.

## 11. DIVERSE GATE VIBRATIONS AND OTHER DYNAMIC EFFECTS

In the storm surge barrier in the Ooster Schelde, which is actually in the final stage of design and the first stage of construction, vertical lift (sliding) gates of 6 - 12 m height and 41 m span will be used. To permit independent placement of the gates and the sills and masks, the gates are positioned to the seaside of the sills. (Were they positioned on the landside, strong wave forces from below could be exercised on the masks.) A wide leak gap is accepted, which ranges between 6 cm under load and 15 cm when unloaded.

The mechanism of the rather strong dynamic flow behaviour found in an elastic similarity model (Fig. 11.1) cannot be explained in an exact way, but is most probably related to the flow capacity, which varies considerably with small changes of the upper (sea-)water level. When the flow separates at the upstream gate (girder) edge, the capacity is greater than when separation occurs at the lower (downstream) edge. Maximum capacity is reached when flow reattachment takes place exactly at the upstream edge of the mask bottom, just beyond the point of maximum flow contraction. So, at a rising upper level the discharge capacity increases and at a dropping upper level it decreases, and this occurs rather abruptly. Moreover, at greater water level oscillations there are still other effects. For instance, at a very low upper water level the mask is no longer touched by the flow and no contraction occurs. Theoretically, a mechanism of

self-sustained water level oscillations is possible, similarly as has been formulated by Streeter and Wylie [4] for self-sustained shock waves (see Par. 4 and Fig. 4.4 of this paper): a self-sustained oscillation can theoretically occur when an increase of the upstream head causes a decrease of discharge.

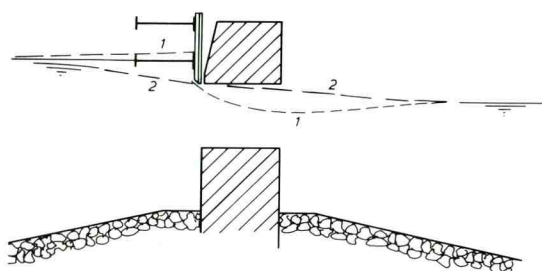


Figure 11.1 Flow instability at vertical-lift gate of Ooster Schelde barrier

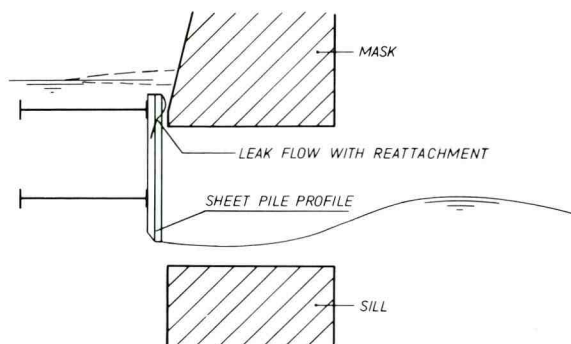


Figure 11.2 Ooster Schelde barrier: vibrations of gate, mask and sill due to fluctuating gap size

When the same gate is nearly closed (see Fig. 11.2), intense vibrations (bending as well as torsion) of the gate and the mask have been found in the elastic similarity/hydraulic model. Probably, the point of maximum flow contraction was situated near the upstream end of the gap passage, a condition which according to the instability indicator is sensitive to vibration. (See the example of Fig. 4.6.) The solution was found in providing the concrete mask with a lip at the edge.

When the 30 m span wheel gate (initial design) described in Chart B and discussed in Paragraphs 4 and 8 was nearly closed and the water levels were such that the upper wheel was on the point of being unloaded, a strong rotational vibration occurred, centered on the lower wheel shaft. In the final design, the gate became a sliding gate and thus the problem was eliminated.

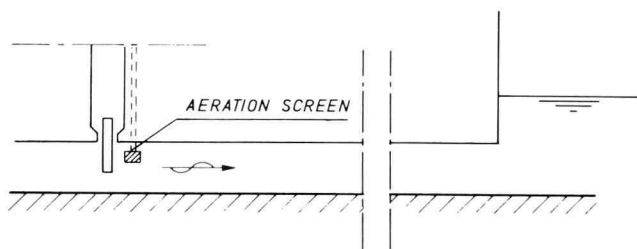


Figure 11.3 Water-hammer effects due to air suction at closing gate

became much lower than the static water pressure in the downstream pool (even lower than the atmospheric pressure), the water flow was decelerated and then reversed. With an initial head difference of 20 m, a water-hammer shock of 110 m water column was recorded.

In a downstream lock culvert of a high-head lock, aeration tubes with screen were installed to suppress gate-induced cavitation (Fig. 11.3). A pressure cell was mounted in the ceiling of the culvert. When the culvert valve was closed, inertia kept the water flowing and air was collected near the gate. As the pressure in this elastic air cushion

### Conclusions:

- The following design criteria can be deduced from the examples given.
- Play in pivots, hoist chains, articulation points, guide wheels, etc. must be preloaded in one definite direction.
  - Free-surface flow can cause considerable changes in flow characteristics

when the surface is oscillating near girders, ceiling, etcetera. Whenever possible, gates should be shaped in such way that a well-defined flow pattern is obtained.

- In culverts, free-surface flow and total submersion are both acceptable, but not situations in between. Oscillating flow surfaces should never be able to hit structural surfaces parallel thereto; nor should a moving or oscillating water surface be allowed near dead corners, as this can cause water-hammer shocks. This holds true for free surfaces related to both air and cavitation pockets, and for whether the free surface oscillation is due to unstable hydraulic jump, wind waves, or water column separation.

## 12. DIFFICULTIES WITH VIBRATION MODELS DUE TO REDUCED REYNOLDS NUMBER

When cylindrical stop logs are used in flow, they show several disadvantages:

- Vortex shedding results in forces of extreme magnitude.
- When they are lowered, there is high pressure underneath (the upstream water is stagnant in the dead-water zones) and the pressure on top is low because flow separation takes place far beyond the point of lowest pressure (due to a regain of pressure head); as a result, the log can be lifted again by the flow.
- Cylinders can roll.

In practice, circular cylinders cannot be lowered in flow; they bump, dance, and even jump out of the water. Still, there is the economic advantage of using commercial tubes. Investigation in our laboratory showed that this is possible when a longitudinal fin is applied so as to give a downward hydrodynamic force; but then rotation of the log must be prevented by means of wheeled slot blocks. There remained a small instability when a log was lowered onto a preceding one (see also Fig. 12.1).

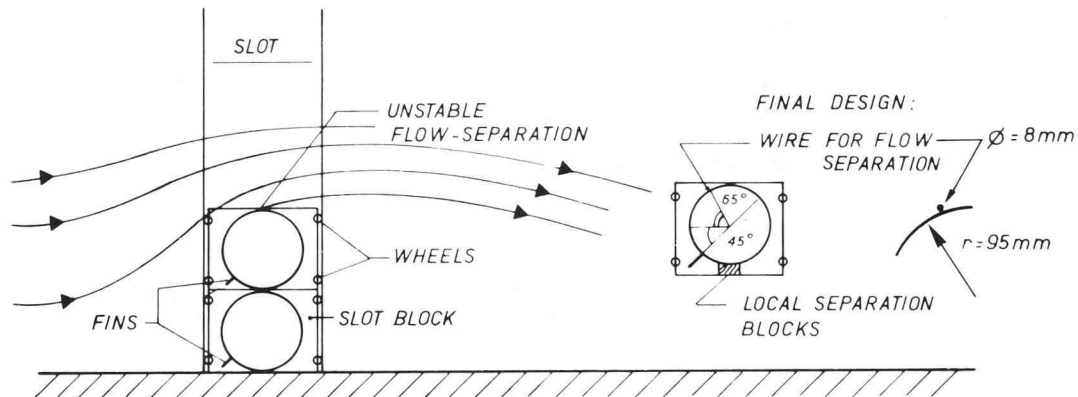


Figure 12.1 Vibration of circular stop logs by retarded flow separation

A prototype experiment showed that the design did not work; so the model result proved invalid. The cause was found by looking into the width of the vortex zone at subcritical (model) and supercritical (prototype) Reynolds numbers: in the model, flow separation took place much farther upstream than in the prototype and low pressure on top of the log did barely occur. The solution for obtaining the same favourable condition in the prototype was found in welding a wire on the tube slightly upstream of the point of flow separation in the model. The optimum position of the wire was determined with a model placed in a closed high-velocity tunnel to obtain a relatively high Reynolds number.

## Conclusions:

- Stop logs must be designed carefully, because vertical forces tend to be important compared to the weight of the log.
- Unstable flow separation should be prevented, not only because it makes hydraulic models less reliable, but especially because surface irregularities (varying from millimetre-size fabrication roughness to centrimetre-thick mussel growth in salt water) can strongly influence the flow pattern; initial turbulence can also strongly change the flow character.

## 13. DESIGN CRITERIA DERIVED FROM EXPERIENCE AND THEORY

Recollecting the conclusions of the foregoing, we can formulate the following design criteria for gates:

1. To prevent self-excitation
  - a in cases of vibration modes in which the gap size fluctuates, suction forces (in general: forces tending to close the gap) should be prevented and the rigidity and/or structural damping should not be too low;
  - b in all cases unstable flow separation and/or reattachment zones should be prevented;
  - c low-pressure regions should preferably be vented by admitting air or water from a high-pressure region;
  - d the width of leak gaps should be at least 1.5 times (preferably 2 times or more) the width of the gate edge;
  - e when play is of influence, no change of force direction should be permitted; and
  - f slender stop logs and gates should be carefully designed so that static and dynamic loads do not prevail over their weight.
2. Resonance frequencies of gate hoist systems and gate members should be well above the dominant excitation frequencies.
3. Water surfaces, unstable because of turbulence, waves, hydraulic jump, water column separation or cavitation, should have no opportunity to hit structural surfaces, especially when these are parallel to the water surface or have dead corners.

It is important to note that when dominant vibration modes are considered, coupling between vibration modes due to added-mass effects and to self-excitation mechanisms has to be taken into account. Moreover, shapes can be influenced by wear, growth of algae and mussels, etc..

## 14. FINAL REMARKS

From this paper have been excluded a few instances of nappe oscillation to which classical remedies, such as splitter plates, have been applied.

Actually, at the University of Karlsruhe, a systems approach is being developed to interrelate all types of aero- and hydro-elastic vibration mechanisms. I hope that this symposium will bring together a lot of information and also that this paper has contributed elements to this approach.

This paper is the result of many design-orientated studies and model investigations in the Delft Hydraulics Laboratory. Most of these projects have been done in close cooperation with the design offices of the Dutch Ministry of Public Works, who have made possible the development of advanced techniques, using expensive and complex combined hydraulic/vibration models (single-oscillator models and continuous elastic similarity models). A few years ago, a general research programme has been set up by this Ministry to improve gate design criteria, and largely thanks to this programme our theoretical base and understanding of vibration mechanisms has been expanded.



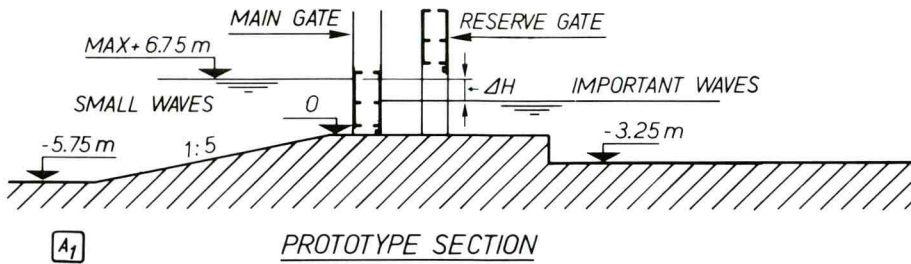
## 15. REFERENCES

1. Kolkman, P.A., "Self-Exciting Gate Vibrations", Invited lecture 17th Congress of Int. Ass. of Hydraulic Research Aug. 1977, Baden-Baden; also Delft Hydraulics Laboratory Publ. 186.
2. Lamb, H., "Hydrodynamics", 6th Ed. Cambridge University Press (1932).
3. Zienkiewicz, O.C., Nath, B., "Analogue Procedure for Determination of Virtual Mass", Proc. of Am. Soc. of Civil Eng.; Journal of Hydr. Div. Sept. 1964 HY5, pp. 69-81.
4. Streeter, V.L., Wylie, E.B., "Hydraulic Transients", McGraw-Hill Book CY (1967).
5. Miller, C., "Ein Beitrag zur Bestimmung des Schwingungserregenden Kräfte an unterströmten Wehre", Inst. f. Wasserbau, Univ. Stuttgart, Publ. 42 (1977).
6. Kolkman, P.A., Vrijer, A., "Gate Edge Suction as a Cause of Self-Exciting Vertical Vibrations", 17th Congress of Int. Ass. of Hydr. Research Aug. 1977, Baden-Baden, Paper C49; also Delft Hydr. Lab. Publ. 188.
7. Hardwick, J.D., "Hydraulic Model Studies of the Rising Sector Gate conducted at Imperial College", Conf. on Thames Barrier Design Oct. 1977, London; Publ. Inst. of Civ. Eng. Paper 12, pp. 133-143.
8. Kolkman, P.A., "Flow-Induced Gate Vibrations", Thesis Delft Univ. of Technology; also Publ. 164 of the Delft Hydraulics Laboratory (1976).
9. Meyers, P., "Numerical Hull Vibration Analysis of a Far-East Container Ship", Netherlands Ship Research Centre TNO Report 195 S (1974).

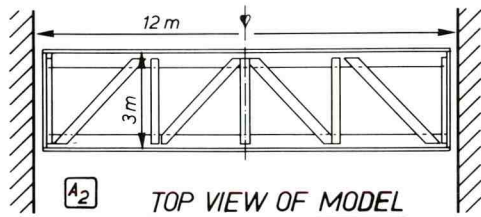
CHART A

VERTICAL LIFT GATE

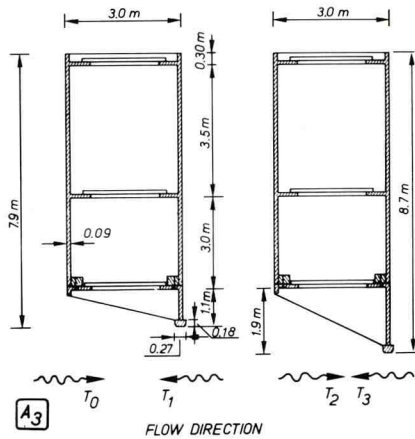
(Section model 1:30; dimensions etc. in proto-value)



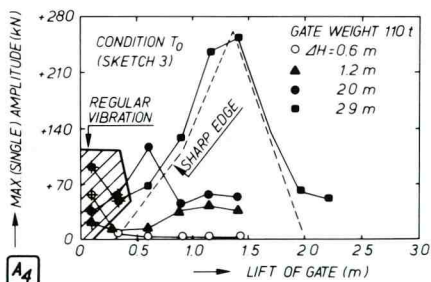
**Problem:** In a single-oscillator model (only vertical vibrations) of Volkerak sluice gates, strong vibrations occurred (max. force ampl. = 28 tonf). Total weight of 30 m span gate = 120 tonf (120 x 10<sup>4</sup> N).



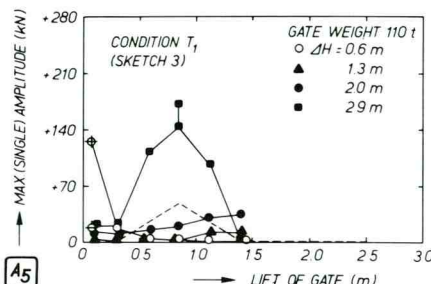
**Geometry:** Sketches 1-3; the 11.9 m long mid-section was reproduced in model.



**Conditions:** Upstream head 6.75 m (above bottom);  $\Delta H = 0.6 - 2.9$  m. Tests to decide if double-plate gate was acceptable. Vibrations at small openings (due to local edge geometry) were not considered, although they did occur. Great preference for smooth double-plate gate (wave forces low) with one plate extended at important wave side ( $T_0, T_2$ ). Final check of design later in continuous elastic model (Chart B).



**Structural dynamics:** Model suspended in horizontal leaf springs; 11.9 m long gate section with  $m = 47$  ton; elastic suspension  $K = 20.2 \times 10^6$  N/m (2020 tonf/m). Resonance freq. dry 3.3 c/s (in water 2.3 - 3 c/s); negligible damping.



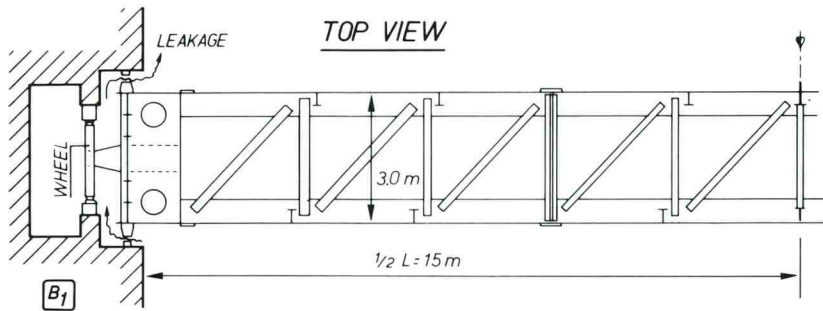
**Vibrations:** Small openings (up to 0.2 m): regular vibration. Greater openings:  $T_0$  condition was worst (less regular vibration), see Sketch A4 (forces are for whole 30 m span gate). For  $T_1$  see Sketch A5.  $T_2$  also showed rather great amplitudes (210 kN at 1.2 m lift).  $T_3$  had only 50 kN force ampl. (two peaks: at lift 0.8 m and 2.7 m). Mechanism: fluctuating gap theory (paper Par. 5) or unstable flow reattachment (paper Par. 10).

**Decision:** Double-plate solution with extended edge (Sketch A3,  $T_3$ ) was chosen, although at high openings waves can slam against the lower girder.

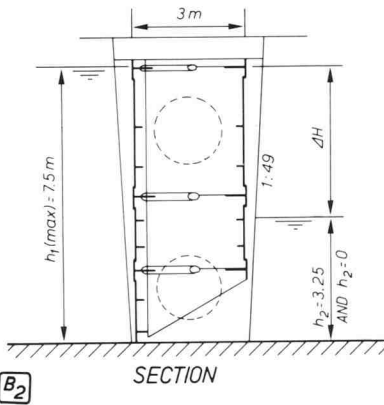
**References:** See Paragraph 4 of this paper.

CHART B

VERTICAL LIFT GATE  
(Hydraulic/continuous elastic model 1:25;  
all dimensions in proto-value)



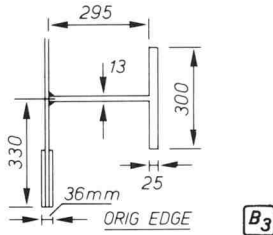
Problem: Check of final design of Volkerak sluice gates (see also Chart A) revealed vibrations at nearly closed position (the gate was designed with a leak gap in "closed" position).



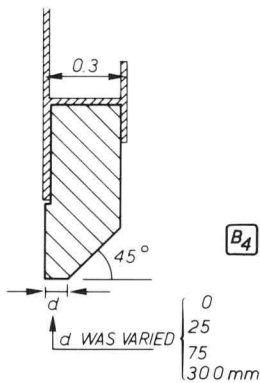
Geometry: Double-plate vertical lift gate, Sketches B1-B3; original design with wheels.

Conditions: Downstream water depth  $h_2 = 0$  and  $h_2 = 3.25$  m in most tests. Upstream water depth  $h_1$  variable with max. 7.5 m. Original design as wheel gate and with edge as shown in B3.

Structural dynamics: Mass 120 tons, hoist rigidity  $2 \times 2.5 \times 10^6$  N/m. Bending rigidity: 3 girders, each  $E \times I = (2.1 \times 10^{11}) \times (0.124) = 26 \times 10^9$  N/m<sup>2</sup>; under dynamic conditions model showed 40% more rigidity. Tests without wheels (to suppress damping) and with a pair of leaf springs for only vertical freedom revealed vibrations of type I.



Vibrations, type I (edge, see B3): Regular vibrations starting vertically (2.9 - 3.5 c/s) and later sometimes (and intense) horizontally. Wave pattern parallel to gate (vert. vibr.) or waves generated at corners (hor. vibr.); see paper Figure 4.5. When  $h_2 = 0$  and  $\Delta H > 2.75$  m, vibrations started. Intense horizontal vibration at  $\Delta H \sim 3.2$  m, disappearing at  $\Delta H = 3.75$  m.



When  $h_2 = 3.25$  m, vibrations starting at  $\Delta H = 3.25$  m and increasing with  $\Delta H$ . Gate edge thickness variations (see B4):  $d = 0, 25, 75$  and  $300$  mm. Critical positions at gap width  $\delta = 0.7 - 1.5 d$ . When  $d = 300$  mm, vibrations started already at  $\Delta H = 1.25$  m. When  $d = 0, 25$  or  $75$  mm and  $h_2 = 3.25$  m no vibrations, but for  $h_2 = 0$  and  $\Delta H = 3.5$  m vibrations also started. Vibrations stopped when vertical friction at the abutments was introduced, or when leakage in slots was nearly blocked. Mechanism: probably unstable flow separation and/or reattachment (paper Par. 7 and 10).

Vibrations, type II: When  $h_2 = 1.75$  m,  $h_1 = 3.25$  m and upper wheel just unloaded (gate nearly closed), strong horizontal vibrations and waves parallel to the gate were observed.

Final gate design: Sharp edge ( $d = 10$  mm); a minimum gap width of  $\delta = 30$  mm at "closed" position; stiffening girder near edge moved to higher position. Wheels removed (slide gate).

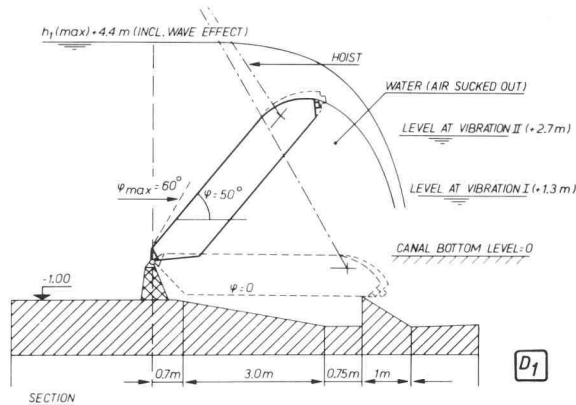
References: See CHART A, and Paragraph 4 of this paper.



CHART D

FLAP GATE

(Hydraulic/vibration model 1:15;  
dimensions etc. in proto-value)



D1

Problem: Emergency gate, which must always be ready to be closed in case of dike rupture. Flow direction normal (as in Sketch D1) or reverse. Model tests showed extremely intense vibrations (rotational) when both downwater  $h_2$  was rather high and nappe was thick, such that air under nappe was sucked away. Nappe spoilers preferably not to be used (ship's anchors).

Geometry: Sketches D1 and D2, span 36 or 50 m, hoist at one side. Rectangular-toothed crest to prevent nappe

vibration at small nappe thickness; flow deflection blocks to keep flow attached at reversed flow direction (extra torque, but safety against vibration).

Flow conditions: Normal canal level +3.7 m; but during closing lower, and when nearly closed higher due to translatory waves. Max. upstream level  $h_{max} = +4.4$  m. During vibrations  $h_1 = h_{max}$  and  $h_2 = +1.3$  m (vibration I) and  $h_2 = +2.7$  m (vibration II). Other h-values not checked.

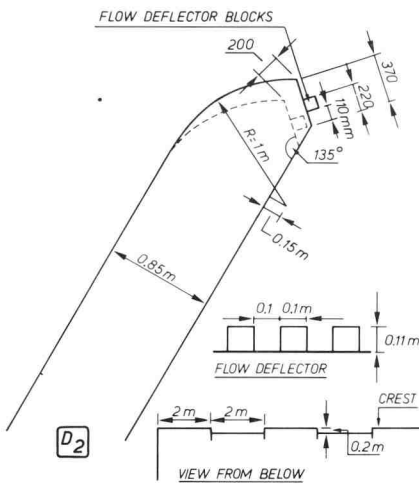
Structural dynamics: In the model a 12.5 m gate section was tested; gate filled with water; polar mass of this section (dry)  $I_p = 0.2 \times 10^6 \text{ kgm}^2$ . Elastic hoist with variable rigidity.

Vibrations:

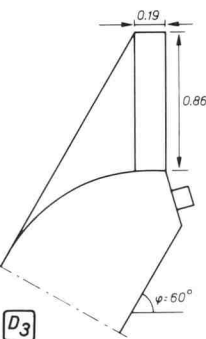
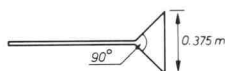
Vibr. I, res. freq. dry 3.5 c/s, in flow 1.3 c/s  
Vibr. II, res. freq. dry 5.2 c/s, in flow 1.7 c/s.  
Both vibrations at  $40^\circ < \phi < 55^\circ$  (max. at  $\phi = 50^\circ$ ).  
Max. amplitude of 12.5 m section was  $1.25 \times 10^6 \text{ Nm}$  torque. Mechanism: flow-contraction fluctuation, see Paragraph 7 of this paper.

Cures: Aeration pipes (one must always remain unsubmerged) or nappe spoilers. Second solution applied: one spoiler near each abutment (Fig. D3). Sufficient condition is that air remains under nappe; this in contrast to thin oscillating nappes, where more aeration is needed to prevent pressure oscillations.

References: See Paragraphs 6 and 7 of this paper.



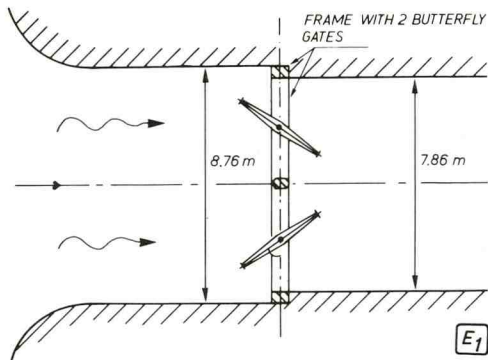
D2



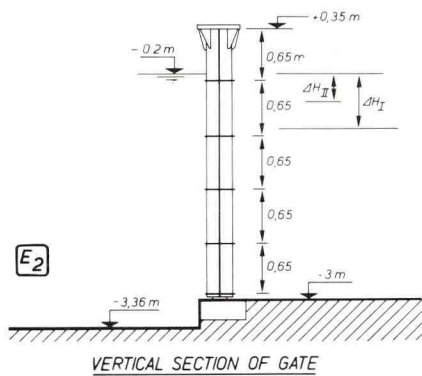
D3

BUTTERFLY GATES

(Hydraulic vibration model 1:10;  
dimensions etc. all in proto-value)

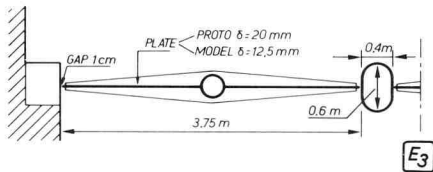


Problem: In a row of old navigation locks at Muiden one lock is adapted for sluicing. For monument conservation reasons, 2 butterfly sluicing gates in a steel frame are hidden under a fixed bridge. The gates consist of a plate with horizontal stiffening ribs (spacing 0.65 m). In "closed" position ( $\phi = 0 - 3^\circ$ ) a leak gap was initially accepted. In this position there was strong plate vibration (vibration I), both audible and with wave radiation. The same occurred at  $\phi = 50^\circ$  (vibration II).



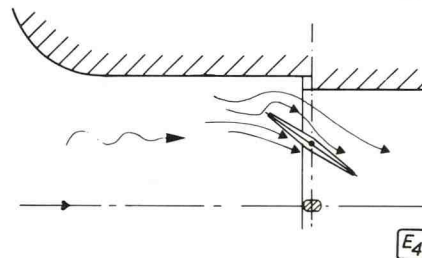
Remark: The model had two elastic elements scaled down: the torsion rigidity of the shaft and the bending rigidity EI of the plate. For this reason, the model thickness of the plate does not completely correspond to prototype values. Mass was not corrected because added mass was considered strongly dominant.

Geometry: Sketches 1-3.

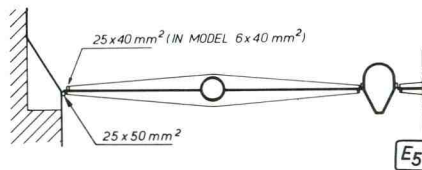


Flow conditions wherein vibrations occurred: Upstr. water level about -0.2 m., head difference  $\Delta H$  up to 2 m. Precise data on  $\Delta H$  at which vibration started not available, but at 0.7 m vibration I was experienced; for vibration II this was 0.35 m.

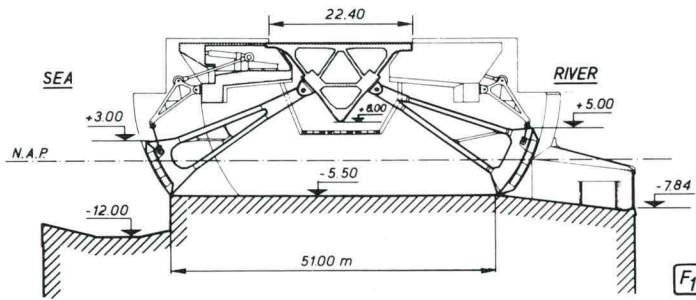
Structural dynamics: Plate in prototype 20 mm steel; in model 12.5 mm (proto-value) brass.



Vibrations: Both vibrations were measurable with a torque meter; unknown magnitude. Vibrations were audible, with frequency 50 c/s (in the model 150 c/s). Vibration I is due to unstable flow separation; vibration II occurred just in the  $\phi$  region where flow wavered at reattachment, see Sketch 4 and Paragraphs 8 and 9 of this paper.



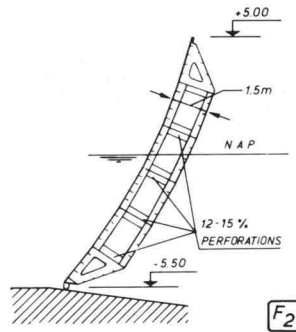
Cures: See Sketch E5: a. stiffening ribs on the plate (thinner ribs were tried but were not effective); b. seats at the centre post and abutments to press the gate against in closed position; c. bevelling of the frame so that the gap widens quickly when opening the gate.



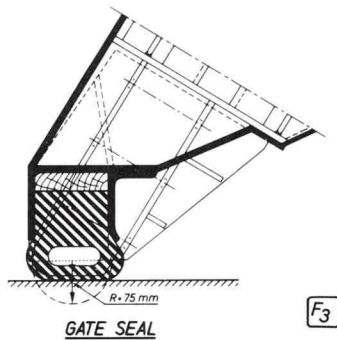
**Problem:** Vertical (= tangential) vibration of river gates of Haringvliet sluices when raised between 1 and 2 m, or between 3 and 4 m; flow from river, sea gates open.

**Geometry:** Sketches 1-3. Gate span 56.5 m. Struts supporting gates from bridge girder have 14.8 m spacing.

**Flow conditions during vibrations:** River level between NAP and NAP +0.5 m; sea levels 0.5-2 m lower.

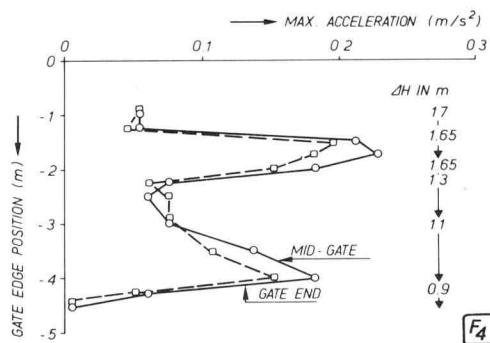


**Structural dynamics:** Weight of gate (= hoist force in dry condition) 520 tonf ( $520 \times 10^4$  N). Hoist rigidity (of the 2 hoists together)  $115 \times 10^6$  N/m in closed gate position and somewhat less when raised. Resonance frequency at closed position: dry,  $f_{res} = 2.3$  c/s; at water level -4 m,  $f_{res} = 2.4$  c/s; at -2 m,  $f_{res} = 2.1$  c/s; at +0.3 m,  $f_{res} = 1.95$  c/s.

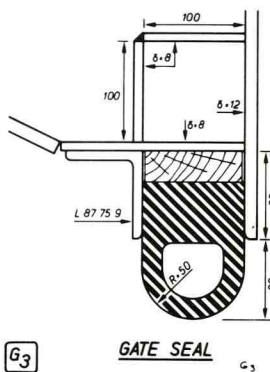
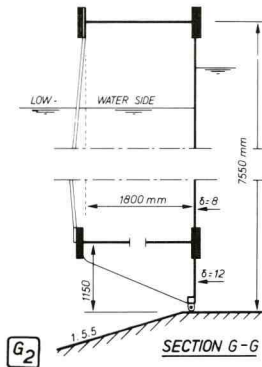
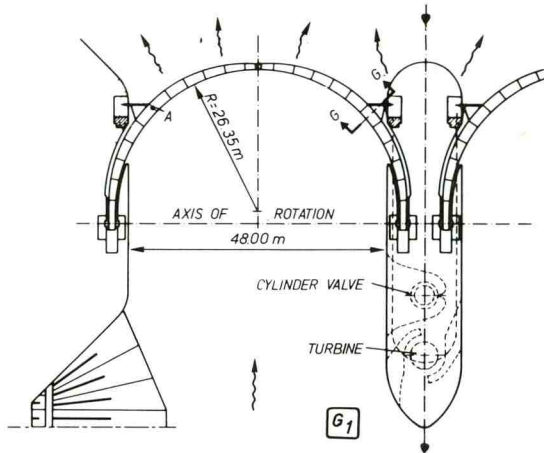


**Vibration:** Regular vibration, frequency between 2 and 2.5 c/s (first natural mode with roughly hoist = spring, gate = mass). Typical experience during one test period: Sketch F4. Max. acceleration amplitude  $\hat{y} = 0.3$  m/s<sup>2</sup>, both when gate was raised 2 m and raised between 3.5 and 4 m. Vibration amplitude  $\hat{y} = \hat{y} : \omega^2 = 1.8$  mm for 2 m gate opening and 1.2 mm for 4 m opening. Vibration mechanism: fluctuating gap theory (see paper Par. 4) or unstable flow reattachment (see paper Par. 10).

**Cures:** No cures tested.



**References:** See Paragraphs 9 (Fig. 9.1) and 10 of this paper. Structural description: "The Haringvliet Sluices", Rijkswaterstaat Communications Nr. 11, 1970 (Ministry of Public Works of The Netherlands).



Problem: At gate lift (midgate) of 0.8 - 1.1 m, local plate vibrations occur near section G. Wave radiation is observed locally.

Geometry: Sketches 1-3.

Conditions: Bottom -4.5 m, downstream level -0.5 to +2.0 m, upstream level +2 to +3 m. During operation, when  $\Delta H$  is greater than about 1 m, vibrations occur. For flow pattern and geometry at critical opening see Sketch 4.

Structural dynamics: Local plate thickness  $\delta = 12$  mm in lower part of the gate. The beam in which the seal is clamped has  $I = 12 \times 10^{-6} \text{ m}^4$ . The seal beam (incl. added mass) between supports (3.7 m spacing) has an estimated resonance frequency of 10 - 15 c/s.

Vibrations: Exact data not available; frequencies about 12 - 20 c/s, local gate lift 0.45 - 0.55 m. Sometimes vibrations regular, sometimes "breathing". Mechanism: unstable flow separation. See also Paragraph 6 of this paper.

Cures: Normally, both gates are raised symmetrically; at critical gate openings one gate is somewhat lowered and the other raised. Sharper edge would be preferable.

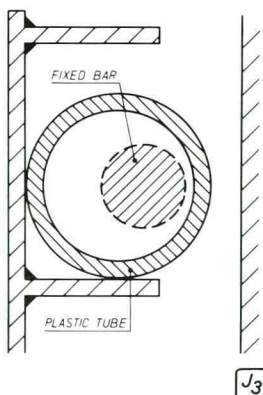
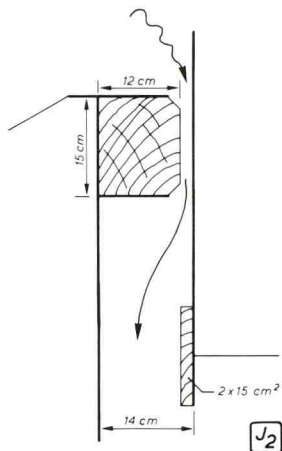
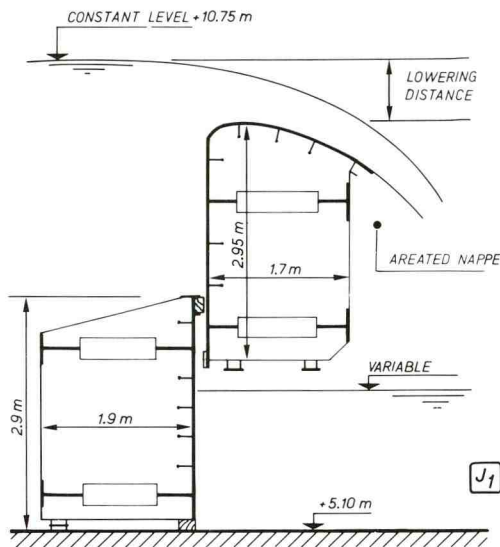
References: See Paragraphs 6 and 7 of this paper. Kolkman, P.A. "Flow-induced Gate Vibrations", Publication 164 of the Delft Hydraulics Laboratory, 1976.





CHART J

DOUBLE-LEAF (STONEY) GATE  
WITH SEAL BEAMS BETWEEN LEAVES



Problem: When the upper gate was lowered more than 0.6 m, combined horizontal and torsional vibration of both leaves started. Vibrations (like a heavy engine in a ship, about 3 c/s) were alarming. After a lowering of  $\Delta H = 1.6$  m nobody dared to go any further because of increased trembling.

Geometry: Sketches 1 and 2. Span between wheels of upper gate 17.6 m, and of lower gate 18.8 m. Width of flow section 17 m. Normally, the lower gate remains on the bottom, but at high river discharge both leaves are taken out.

Flow conditions: Sketch 1. Low turbulence upstream. Nappe aerated from both sides. Constant upstream water level.

Operating conditions: Vibrations observed when lowering of upper leaf from 0.6 to 1.6 m; at latter value further lowering was forbidden. Design condition: variation between completely closed (raised) and completely open (lowered) position of the upper leaf.

Structural dynamics: Horizontal rigidity of each girder of lower gate  $I_{yy} = 0.03 \text{ m}^4$ , and of upper gate  $0.018 \text{ m}^4$  with an extra influence of the crest rigidity of  $0.007 \text{ m}^4$ . The torsional rigidity at the first harmonic vibration follows completely from these horizontal rigidities, but is not calculated. Weight of the upper leaf 22.5 tons and weight of the lower leaf 24 tons.

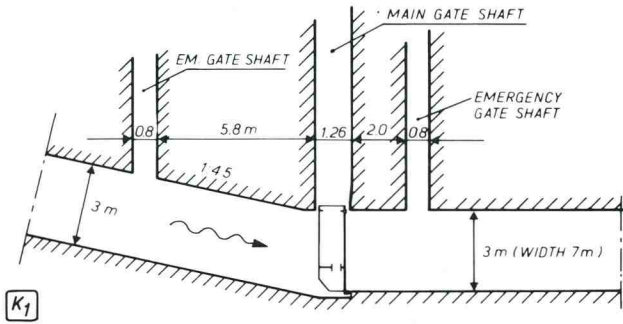
Vibration: Not measured, only felt with a stick; 3 c/s vibration; combined torsion and bending (in the first harmonic) of both leaves. (Single) amplitudes up to 2.5 mm at 1.6 m lowering. Hoist chain vibration amplitude a few cm.

Cures: Type of vibration follows from fluctuating gap width theory (Par. 5 of this paper). Vibration stopped when leakage flow was provisionally sealed with a plastic rain pipe. Final solution Sketch 3. Theoretical considerations and use of the instability indicator (see conclusions of Par. 4 of this paper) reveal that another solution is to exchange the two seal beams (and fix the thick one to the upper leaf).

Reference: See Paragraphs 4 and 5 of this paper.

VERTICAL-LIFT CULVERT GATE WITH RELEASE SYSTEM

(Hydraulic model 1:15; all dimensions etc. proto-value)



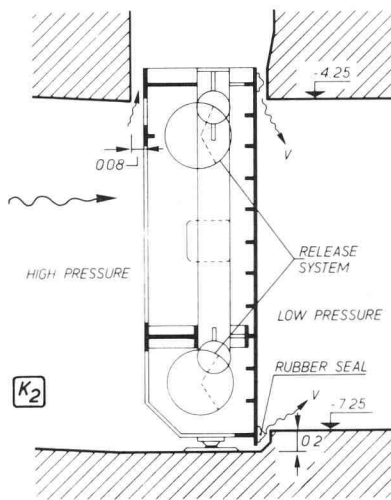
**Problem:** During model investigation it was found that, when the gate is closed but released from its seat, intense horizontal vibrations occurred; amplitudes were probably limited because the gate hit its seat.

**Geometry:** Sketches 1, 2 and 3. In the model, the wheels of the gate were replaced by lateral arms so that the gate could be supported by

4 vertical leaf springs to permit horizontal and rotational vibrations with low damping. Slot geometry was kept realistic; the leaf springs were submerged.

**Flow conditions:** Completely submerged; upstream level 9.3 m above culvert bottom.

**Operating conditions:** Front seal applied (with a release system) to guarantee absolute water tightness in closed position. Maximum head difference 5.5 m, which is the determining condition at the moment when the gate is just released and vibration commences.



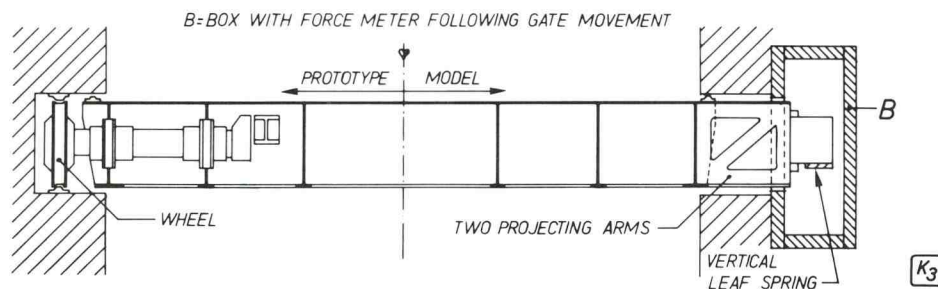
**Structural dynamics:** Model gate designed as single oscillator. Horizontal rigidity  $108 \times 10^6$  N/m; gate mass (incl. release construction, hoist bars, etc.)  $18 \times 10^3$  kg. Horizontal bending vibration in main girders and wheel shaft is feared for in prototype;

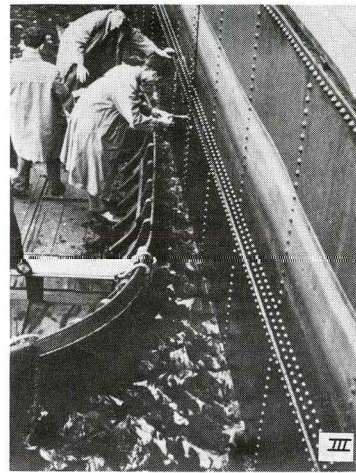
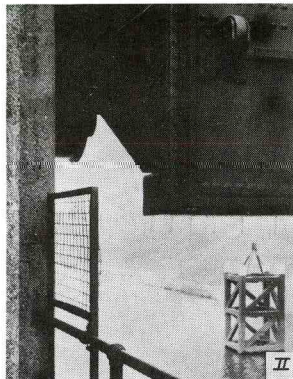
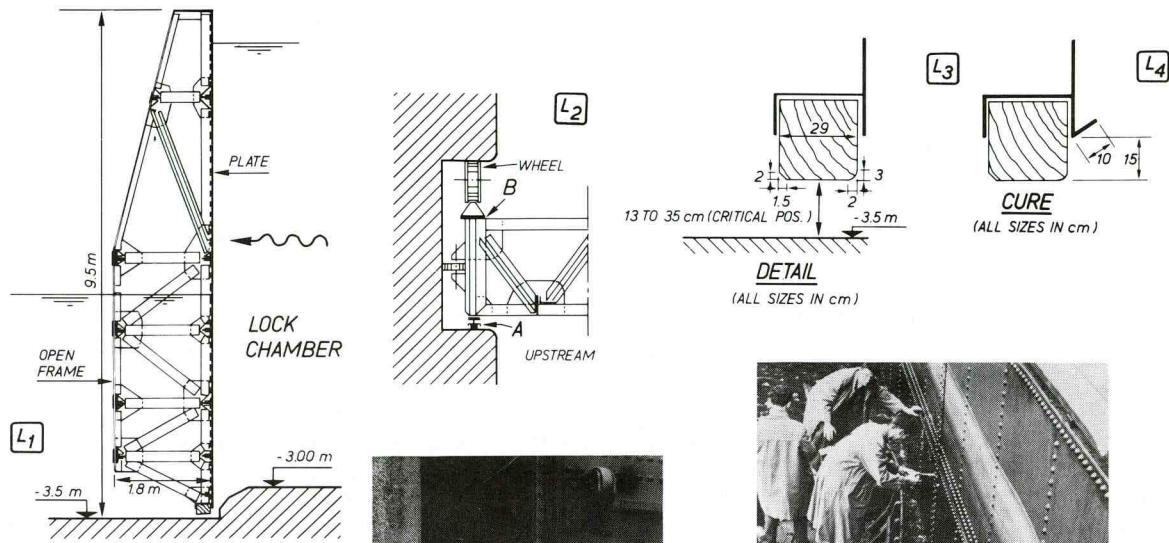
model was only schematically representative (Fig. 4.2 of this paper).

**Vibration:** When gate was released with a small opening: very intense horizontal vibrations. Vibrations started purely incremental, max. amplitude probably when gate touched its seat. Excitation mechanism: see bath-tub plug vibration in Paragraph 5 of this paper. Resonance frequency of horizontal gate vibration was in general 6 - 10 c/s, but at nearly closed position 2.5 c/s because part of the culvert volume then acted as added mass volume.

**Cure:** Release system should give minimum real gap width of 15 mm, taking into account reshaping of the squeezed rubber seal.

**Reference:** See Paragraphs 4 (Fig. 4.3) and 5 of this paper. For the total lock structure: Kolkman, P.A. and Slagter, J.C., "The Kreekrak Locks on the Scheldt-Rhine connection", Delft Hydraulics Laboratory, Publication 160 (1976).





Problem: Lock at Lith; emptying by raising gate. Vibration after a revision: renewal of wooden seal beam and truing of main wheels (1 cm radius reduction). Although strip B (Sketch 2) was adjusted, seal beam A (normally

reduced damping) started leaking because its rubber was worn off 2 cm; this probably

Geometry: Sketch 1. Gate span between walls 14 m. Retaining plate and side seal beams at upstream side. Wooden lower seal: Sketch 3. Details: Plates I and II.

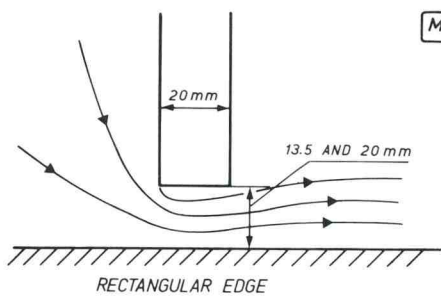
Boundary conditions: Wheel gate; varying lock water level during emptying.

Operating conditions: Upstream level before gate raising: +4.5 m. Downstream level varying during tests between +1.05 and +1.4 m. Critical gate openings 0.13 - 0.35 m (most critical 0.25 m). When  $\Delta H < 1.9$  m, vibration stopped.

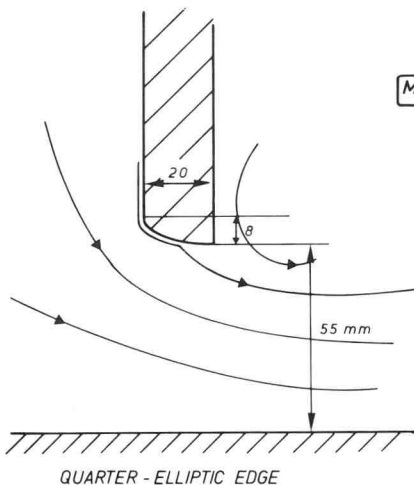
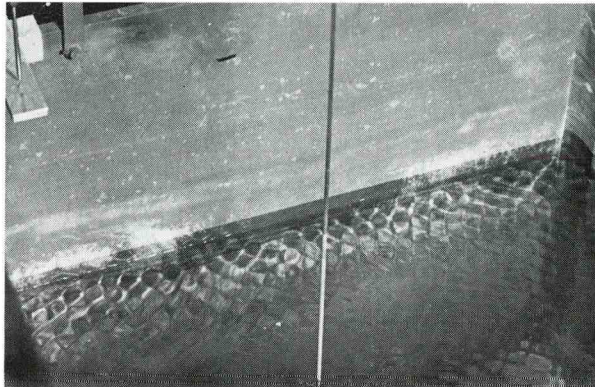
Structural dynamics: Gate mass 90 tons. Total horizontal bending rigidity  $EI = 250 \times 10^{12}$ . Gate is cable-suspended ( $\Sigma K = 1.3 \times 10^7$  N/m), but is also counterbalanced. Rigidity between gate and counterweight:  $k = 1.2 \times 10^7$  N/m (both k-values estimated from cable data).

Vibrations: Starting vertically (wave crest parallel to gate plate), but then becoming intense as horizontal vibration (pattern of intersecting waves;  $f$  between 4.8 c/s and 5.2 c/s; only first harmonic vibr. involved. Max. (single) vertical ampl. 0.25 mm; horizontal mid-gate ampl. 5 mm. Vertical vibr.: fluctuating gap theory (Par. 5 of this paper). Horizontal vibr.: hypothesis of flow contraction fluctuation (Par. 7).

Cure: 1 m spaced, 0.4 m long pieces of steel angle bar (Sketch 4) to prevent: 1) complete synchronization of vortex street, and 2) a uniform critical gate position over the entire length. At the middle of gate, 2 pieces and at each side one piece were left out for construction reasons.



M<sub>1</sub>



M<sub>2</sub>

Problem: When pressure measurements at gate edge were performed in hydraulic model, strong bending vibrations of the plate occurred. This example is typical of high-frequency edge vibrations at gaps with thin-edged gates.

Geometry: Sketches 1 and 2. The 20 mm plate was about 1 m high and extended above the maximum water surface. Flume width 1 m.

Boundary conditions: Low-turbulence approach flow.

Flow conditions: Upstream depth 0.5 - 1 m, downstream depth 0.1 - 0.8 m, max.  $\Delta H = 0.6$  m.

Structural dynamics: Steel plate 2 cm thick, 1 m high, 1 m wide; secured by wedges which were fixed to the walls. Bottom edge (about 3 cm high) made of Trovidur.

Critical conditions: a) Rectangular edge: lifts of 13.5 and 20 mm were sensitive; 10, 30, 140 mm were not. b) Elliptical edge: only 55 mm lift was tested.

Rectangular edge: vibration started at  $\Delta H > 0.1$  m. At the 13.5 mm lift the following combinations  $h_{up}/h_{down}$  were checked: 0.5 m/0.1 m, 0.5 m/0.3 m, 0.7 m/0.3 m, 0.9 m/0.3 m, 0.7 m/0.5 m, 0.9 m/0.5 m and 1.0 m/0.8 m. At all levels vibrations occurred, the strongest at 0.7 m/0.3 m. At the 20 mm lift the following tests were done:  $h_{up}/h_{down} = 0.5$  m/0.3 m, 0.7 m/0.3 m, 0.9 m/0.3 m, 0.7 m/0.5 m, 0.9 m/0.5 m, 0.9 m/0.8 m and 1.0/0.8 m. At all levels vibration occurred, but at 0.9 m/0.3 m and 0.9 m/0.8 m they were only weak.

Elliptical edge: rather strong vibrations at every tested  $h_{up}/h_{down}$  combination: 1:0 m/0.6 m, 0.6 m/0.2 m, 0.8 m/0.2 m, 0.8 m/0.4 m and 1.0 m/0.4 m, all with a lift of 55 mm.

Frequencies: Not measured; wave length of the cross-wave pattern  $\lambda = 2$  cm, which could indicate 11 c/s; but there was a rumbling noise of probably 20 c/s, which is the calculated first natural frequency of the submerged plate.





p.o.box 177

2600 MH delft

the netherlands